Gajica, G.; Šajnović, A.; Stojanović, K.; Schwarzbauer, J.; Kostić, A.; Jovančićević, B. A Comparative Study of the Molecular and Isotopic Composition of Biomarkers in Immature Oil Shale (Aleksinac Deposit, Serbia) and Its Liquid Pyrolysis Products (Open and Closed Systems). *Marine and Petroleum Geology* **2022**, *136*, 105383. https://doi.org/10.1016/j.marpetgeo.2021.105383.

A comparative study of the molecular and isotopic composition of biomarkers in immature oil shale (Aleksinac deposit, Serbia) and its liquid pyrolysis products (open and closed systems)

Gordana Gajica[a*], Aleksandra Šajnović[a], Ksenija Stojanović[b], Jan Schwarzbauer[c], Aleksandar Kostić[d], Branimir Jovančićević[b]

[a] University of Belgrade, Institute of Chemistry, Technology and Metallurgy – Center of Chemistry, Njegoševa 12, 11000 Belgrade, Serbia; E-mails: gordana.gajica@ihtm.bg.ac.rs, aleksandra.sajnovic@ihtm.bg.ac.rs

[b] University of Belgrade, Faculty of Chemistry, Studenski trg 12-16, 11000 Belgrade Serbia; E-mails: ksenija@chem.bg.ac.rs, bjovanci@chem.bg.ac.rs

[c] RWTH Aachen University, Institute for Geology and Geochemistry of Petroleum and Coal, Lochnerstrasse 4-20, 52056 Aachen, Germany; E-mail: schwarzbauer@lek.rwth-aachen.de

[d] University of Belgrade, Faculty of Mining and Geology, Đušina 7, 11000 Belgrade, Serbia; E-mail: aleksandar.kostic@rgf.bg.ac.rs

Abstract

The molecular and isotopic composition of biomarkers in initial bitumen isolated from immature (0.41 % Rr) oil shale samples (Aleksinac deposit) and liquid products obtained by pyrolysis in open (OS) and closed (CS) systems are studied. The influence of pyrolysis type and variations of kerogen type on biomarkers composition and their isotopic signatures in liquid products is determined. The applicability of pyrolysis type, numerous biomarkers and carbon isotopic compositions ($\delta^{13}C$) of *n*-alkanes in liquid pyrolysates is established. Pyrolysis experiments were performed on two selected samples that showed high content of total organic carbon and hydrocarbon generation potential, but also certain variations in sources/depositional environment of organic matter (type I and mixed type I/II kerogen) within previous research of the oil shales sample set. The biomarker signatures were evaluated using gas chromatography-mass spectrometry (GC-MS) and $\delta^{13}C$ of individual *n*-alkanes in bitumen and liquid pyrolysates. The molecular composition of liquid pyrolysates from the OS is very similar to those in initial bitumen, independently on kerogen type, confirming algal origin of organic matter (OM) deposited in lacustrine environment, even more apparently than results of initial bitumen. Therefore, OS can be useful for assessment of source and depositional environment of OM. Pyrolysis in the CS caused more intense thermal alterations, therefore the source fingerprints sometimes notably disappear. The liquid pyrolysates from the CS have the distributions of

biomarkers similar to those in crude oils. The biomarker maturity parameters showed slightly higher values in the CS pyrolysate of mixed type I/II kerogen in relation to type I kerogen. $\delta^{13}C$ of *n*-alkanes in liquid pyrolysates from the OS are isotopically lighter in comparison to bitumen, independently on kerogen type. Oppositely, in liquid pyrolysates from the CS, they become heavier than in bitumen, indicating the thermal influence on $\delta^{13}C$ signatures, with more pronounced difference for type I kerogen.

* Corresponding author. Phone +381 11 3336 724; Fax: +381 11 2636 061;
E-mail address: gordana.gajica@ihtm.bg.ac.rs (Gordana Gajica)

***Key words**: outcrop oil shale, Aleksinac deposit, organic matter, open and closed system pyrolysis, biomarkers, stable carbon isotope composition.*

1. Introduction

Oil shales are considered as a potential source of energy since they usually contain a large amount of solid fossil hydrocarbons (10^{16} t) bounded in the kerogen (Sert et al., 2009). In addition to the high content of solid fossil hydrocarbons (HCs), a significant feature of oil shales is the high atomic H/C ratio (coal 0.4-1.0; oil shales > 1.7; oil ~ 1.9) and unique composition of organic matter (OM) in relation to other solid fossil fuels (Strizhakova and Usova, 2008). The oil and gas potential of oil shales implies their ability to generate HCs, and depends on the quantity, type and maturity of OM (Tissot and Welte, 1984). As oil shales are commonly immature or at a low degree of maturity, they have the full potential (equal to initial) to produce liquid and gaseous hydrocarbons via technical processing.

The OM in oil shale is present in a variable amount and type, distributed finely and irregularly in an inorganic matrix. The major part of OM is present in the form of an insoluble OM (kerogen), while extractable OM (bitumen) is present in a very low percentage. Although bitumen is present in a small amount, the analysis of biomarker composition of bitumen can provide important information about the origin and maturity of OM, as well as paleoenvironmental conditions that occurred at the time of deposition of the investigated samples (Tissot and Welte, 1984; Peters et al., 2005; Hatem et al., 2016).

On the other hand, kerogen, comprising the major part of oil shale OM, is a complex geopolymer, insoluble in conventional inorganic and organic solvents, and despite of development of numerous methods, its detail analysis still represents the challenge. Pyrolysis is one of the techniques for organic geochemical investigation of kerogen. It represents controlled heating of kerogen in an inert atmosphere, which causes thermal decomposition of its complex structure into lower molecular weight fragments leading to its transformation into soluble OM, which can be further analyzed more easily. The composition of the kerogen can be assessed by analyzing the biomarker composition in pyrolysates obtained by thermal decomposition of kerogen, in the same way as the analysis of biomarkers in initial bitumen (Philp, 1987). In addition to many common characteristics, biomarker composition obtained by pyrolysis of kerogen can notably differ from free biomarkers in bitumen generated during native (geological) maturation (Monthioux et al., 1985; Philp, 1987; Farrimond et al., 1998; Franco et al., 2010). Biomarkers are incorporated into kerogen by covalent bonding (de Leeuw et al., 1989; Hoffman et al., 1992; Adam et al., 1993), as well as by adsorption and occlusion (Cheng et al., 2016; Snowdon et al., 2016). Since it is very difficult to differentiate the bound moieties released by pyrolysis methods from occluded ones (Snowdon et al., 2016), most researches use the term bound biomarkers (including both covalently bound and occluded biomarkers) to represent the products released from macromolecular structures. Due to the protection afforded by their macromolecular hosts, the thermal maturity of bound biomarkers is generally lower than that of their freely occurring counterparts (Rubinstein et al., 1979; Russell et al., 2004; Lockhart et al., 2008; Wu et al., 2013).

The molecular composition of pyrolysates primarily depends on kerogen type and maturity, but also on the type of applied pyrolysis system and the operating conditions (reactor type, temperature, heating rate, pressure, residence time, type and flow rate of inert gas, size of the particles, presence of catalyst, etc.). Many studies have been conducted on pyrolysis experiments in open (Rock-Eval, thermal gravimetric analysis, flash pyrolysis, laser micropyrolysis) and closed (autoclave, Au capsules, microwave) systems using different types of sedimentary rocks and operating conditions (Monthioux et al., 1985; Behar et al., 1992; Pakdel et al., 1999; El Harfi et al., 2000; Yoshioka and Ishiwatari, 2002; Sugden et al., 2005; Pan et al., 2010; Hakimi et al., 2018).

Pyrolysis in an open system (OS) allows liberating biomarkers that are adsorbed and weakly bounded to kerogen and can provide better insight into the nature of kerogen-bound compounds and the types of precursor biomass. Pyrolysis in a closed system (CS) is applied to stimulate kerogen maturation processes after diagenesis, oil and gas generation phase, which would take place upon the geological conditions if sediments have reached greater depths.

During last decade, in addition to aforementioned routine pyrolytical techniques, microscale sealed vessel (MSSV) pyrolysis and catalytic hydropyrolysis combined with gas chromatography–mass spectrometry attracted emerged attention as useful and versatile methods. The MSSV pyrolysis performs in a closed system at lower temperatures (250–350 ^{o}C) over longer time periods (e.g. days) in comparison to the high temperatures (> 500 ^{o}C) and ballistic heating rates associated with flash pyrolysis. Therefore MSSV pyrolysis can provide additional speciation information useful for establishing the structure and source inputs to recent OM (Berwick et al., 2007), although the extended heating times and closed-nature of MSSV pyrolysis may contribute to the cracking of the alkyl side chain of biomarkers and their isomeric rearrangement (Berwick et al., 2010). The catalytic hydropyrolysis is conducted from 300 to 550 ^{o}C using much slower heating rates (e.g. 8 ^{o}C/min) than flash pyrolysis. Metal sulfide catalysts are used to reduce the thermal profile of volatile evolution, thus avoiding the application of very high temperatures which promote secondary processes. Products are rapidly removed from the open-system thermal reactor, which is maintained under high hydrogen pressure (>10 MPa). These conditions support the relatively soft release of pyrolysis fragments, with less structural and isomeric rearrangement in comparison to MSSV pyrolysis (Berwick et al., 2010). Recent modification of the standard MSSV pyrolysis (using tetralin as hydrogen donor and dispersed sulfide molybdenum as catalyst) increased biomarker release from kerogen and reduced secondary cracking of released biomarkers (Wu and Horsfield, 2019).

Compound specific isotope analysis (CSIA) of individual biomarkers (e.g. *n*-alkanes) can be also used to obtain information about source (plants, algae and phytoplanktons differ in the way how they assimilate CO_2 during photosynthesis) and maturity (during maturation processes enrichment in heavier isotope occurs) of OM (Lewan, 1983; Freeman et al., 1990; Schwarzbauer et al., 2013; Strobl et al., 2014).

The samples used for pyrolytic experiments within this study originated from the Aleksinac oil shale deposit, which is the largest and richest oil shale deposit in Serbia (Jelenković et al., 2008).

The molecular composition of aliphatic hydrocarbons, ketones and fatty acid methyl esters, as well as $\delta^{13}C$ values of individual *n*-alkanes in extracted initial bitumen of two immature raw oil shale samples, containing type I and mixed type I/II kerogen, respectively, and liquid products obtained by the open system pyrolysis (OS) and the closed system pyrolysis (CS) are studied. The influence of pyrolysis type and variations of kerogen type on biomarkers composition and their isotopic signatures in liquid products is determined. The applicability of pyrolysis type, numerous biomarkers and carbon isotopic compositions of *n*-alkanes in liquid pyrolysates is established.

2. Material and methods

2.1. Samples

Pyrolytic experiments have been conducted on immature outcrop oil shale samples from the Aleksinac deposit, Serbia (Jelenković et al., 2008). These oil shales were deposited in lacustrine (brackish to freshwater) environment during Lower Miocene, and samples analyzed within this study were taken from the Upper layer of the Dubrava block (Gajica et al., 2017a). Two samples, which have shown the highest total organic carbon, TOC (D16, 29.10 wt. %; D13, 13.19 wt. %) and the highest hydrogen index, HI (D13, 858 mg HC/g TOC; D16, 619 mg HC/g TOC) as revealed by previous investigation performed on the oil shales sample set (Gajica et al., 2017a), were selected for pyrolytic experiments. The selected samples are immature (huminite reflectance, Rr = 0.41 %; Production Index, PI = 0.02), generated a high yield of liquid hydrocarbons (Gajica et al., 2017a, b), but contain different kerogen types (D13 type I; D16 mixed type I/II). Furthermore, the D16 is characterized by elevated sulfur content (6.11 wt. %) and prevalence of carbonates (63.87 wt. %) in mineral matter, while the D13 sample has lower amount of sulfur (0.21 wt. %) and carbonates (33.95 wt. %; Gajica et al., 2017a).

2.2. *Methods*

2.2.1. Analysis of raw oil shale samples

Prior to bitumen extraction, the samples were crushed and pulverized (< 63 μm). Details of bitumen extraction and separation into fractions, as well as gas chromatographic-mass spectrometric analysis (GC-MS) are given elsewhere (Gajica et al., 2017a). Oxygen containing compounds, ketones and fatty acid esters, were also analyzed complementarily to the biomarkers

of the aliphatic fraction due to their structural similarity to *n*-alkanes. *n*-Alkan-2-ones and fatty acid methyl esters were identified in aromatic fraction based on typical ion fragmentograms, *m/z* 58 and 74, respectively.

2.2.2. Pyrolytic experiments on bitumen-free oil shale samples

Pre-extracted, bitumen-free samples containing kerogen and native mineral matrix were used for pyrolytic experiments. Samples were pre-extracted, because the free bitumen, especially its polar fraction containing functionalized hopanoids and steroids, may have been incorporated into the kerogen during pyrolysis (Vu et al., 2008; Wu and Geng, 2016). The temperature of 400 ^{o}C, providing high yields of biomarkers, was chosen according to the literature data (Comet et al., 1986; Lewan et al., 1986; Wu and Geng, 2016, Wu and Horsfield, 2019) and our preliminary performed experiments.

The open system (OS) pyrolysis was performed using Pyrolyser, Model MTF 10/15/130 (Carbolite Limited, Parsons Lane, Hope, UK) at temperature of 400 ^{o}C under a nitrogen atmosphere. The samples were heated from 20 ^{o}C to the final pyrolysis temperature at a rate of 5 ^{o}C/min and the duration of pyrolytic experiments at the final temperature was 4 h. The furnace (15 cm long) was equipped with a quartz tube (inner diameter, 1 cm) that was 4.5 times longer than furnace. The quartz tube was situated within the furnace and equal parts of the quartz tube were outside of furnace. The tube was connected to the nitrogen supply at one side, while the other was connected to a trap (cooled to 0 °C), filled with 20 cm^3 of chloroform, to which the pyrolysis products were transferred by the N_2 flow. Liquid products were collected in cold trap, whereas released gases could not be collected. The sample (~ 1.5 g) was situated in the quartz vessel and the vessel with the sample was transferred into the pyrolysis furnace in the middle of the quartz tube. After cooling the pyrolytic system over night, the quartz tube and solid residue were rinsed with hot chloroform and this extract was combined with the liquid product collected in the cold trap. Chloroform was removed by rotary vacuum evaporator. Liquid product was quantitatively transferred from the flask to small glass bottle using a Pasteur pipette and dried to the constant mass under ambient conditions.

The closed system (CS) pyrolysis was carried out in a stainless steel reactor (autoclave), which was loaded with ~ 5 g of the sample. After loading, the autoclave was sealed, pressurized to ~6 MPa of nitrogen and checked for leaks. When no leaks were detected, the system was purged

three times with nitrogen in order to remove the air. The initial nitrogen pressure was then reduced to 600 kPa. The samples were heated from 20 ^{o}C to 400 ^{o}C at a rate of 5 ^{o}C/min and the duration of pyrolytic experiments at the final temperature was 4 h. During the experiments the temperature was continuously monitored at 30 s intervals using Type J thermocouple. The obtained standard deviations ranged between 0.3 and 0.6 ^{o}C. After the experiments were completed, the reactor was cooled down to room temperature overnight. It was then vented and opened to collect the liquid products and solid residue. Liquid pyrolysis products were extracted using chloroform, by combining thorough rinsing of the autoclave interior and the solid residue with hot solvent. Chloroform was removed by rotary vacuum evaporator. Liquid product was quantitatively transferred from the flask to small glass bottle using a Pasteur pipette and dried to the constant mass under ambient conditions.

The obtained liquid pyrolysates were analyzed using the same procedure as for initial bitumen extracted from the raw oil shale samples (Gajica et al., 2017a).

2.2.3. Compound specific stable isotope analysis (CSIA)

Compound specific stable carbon isotope analysis of individual *n*-alkanes in aliphatic fraction of bitumen and liquid pyrolysates was performed using a gas chromatography-isotope ratio monitoring-mass spectrometry system (GC-irmMS). A gas chromatograph 6980A was linked to a Finnigan Delta Plus XL mass spectrometer equipped with a GCC III combustion interface (Fisons Instruments). Gas chromatographic separation was carried out on a ZB1 fused silica capillary column (30 m x 0.25 mm i.d.; 0.25 µm film thickness). Chromatographic conditions were as follows: 1 µL splitless injection (injector temperature 270°C) at an oven temperature of 60°C, splitless time 60 s, 3 min hold, then programmed at 3°C min^{-1} to 300°C. The helium carrier gas velocity was set to 35 cm s^{-1}. The oxidation oven equipped with a CuO/NiO/Pt-catalyst was set at 940°C. Each isotope ratio determination was run in triplicate. The carbon isotope ratio of the reference gas (carbon dioxide) was calibrated with a certified reference standard purchased from Chiron (Trondheim, Norway) containing *n*-C_{11} (–26.11 ‰ vs. VPDB), *n*-C_{15} (–30.22 ‰ vs. VPDB) and *n*-C_{20} (–33.06 ‰ vs. VPDB). All data presented are expressed relative to the VPDB (Vienna Pee Dee Belemnite) standard. The internal precision of measurements was determined by standard deviations between 0.1-0.4 ‰ with maximum values around 0.8 ‰.

3. Results and discussion

3.1. The molecular composition of aliphatic fraction of initial bitumen and liquid pyrolysates

The gas chromatographic patterns of the aliphatic fractions in bitumen of raw samples and liquid pyrolysates from the open and the closed systems are given in Figure 1, while specific ion chromatograms of *n*-alkanes, ketones, fatty acid methyl esters, steranes and terpanes are given in Figures 2-6. Specific parameters calculated from distributions of mentioned biomarkers are listed in Table 1.

The distribution of aliphatic hydrocarbons in initial bitumen of the sample D13 is characterized by domination of isoprenoids (phytane, β-carotane) and steranes. On the other hand, the distribution of aliphatic hydrocarbons in initial bitumen of the sample D16 is characterized by prevalence of *n*-alkanes, relatively high amount of steranes and hopanes, and the presence of β-carotane in low abundance (Fig. 1a, d). The observed differences in total ion chromatograms (TICs) of aliphatic fractions are consistent with certain variations in sources of OM that are also reflected through the kerogen type, since both raw oil shale samples showed uniform and low maturity.

The distribution of aliphatic hydrocarbons in liquid pyrolysate from the OS of the sample D13 is characterized by high abundance of regular isoprenoid alkanes (C_{16} and C_{18}) and pristene. Such a domination of lower regular isoprenoids is not common in native samples, and it is indicative for notable contribution of algal OM (Fig. 1b; Volkman et al., 2015). Both liquid products from the OS are characterized by prevalence of *n*-alkanes in pairs with terminal *n*-alkenes, which is also indicative of algal sources (Fig. 1b, e; Zhang et al., 2016) and low thermal maturity. The polycyclic biomarkers with sterane and hopane skeleton are clearly visible only in liquid pyrolysates from the OS of sample D13.

n-Alkanes notably dominated in the distribution of aliphatic hydrocarbons in both liquid pyrolysates from the CS,. These liquid pyrolysates also have relatively high content of regular isoprenoid C_{18}, pristane and phytane. On the other hand, terminal *n*-alkenes in liquid pyrolysates from the CS are present in a lower amount than in liquid pyrolysates from the OS (Fig. 1b, c, e, f). This indicates intense secondary processes in the CS compared to OS.

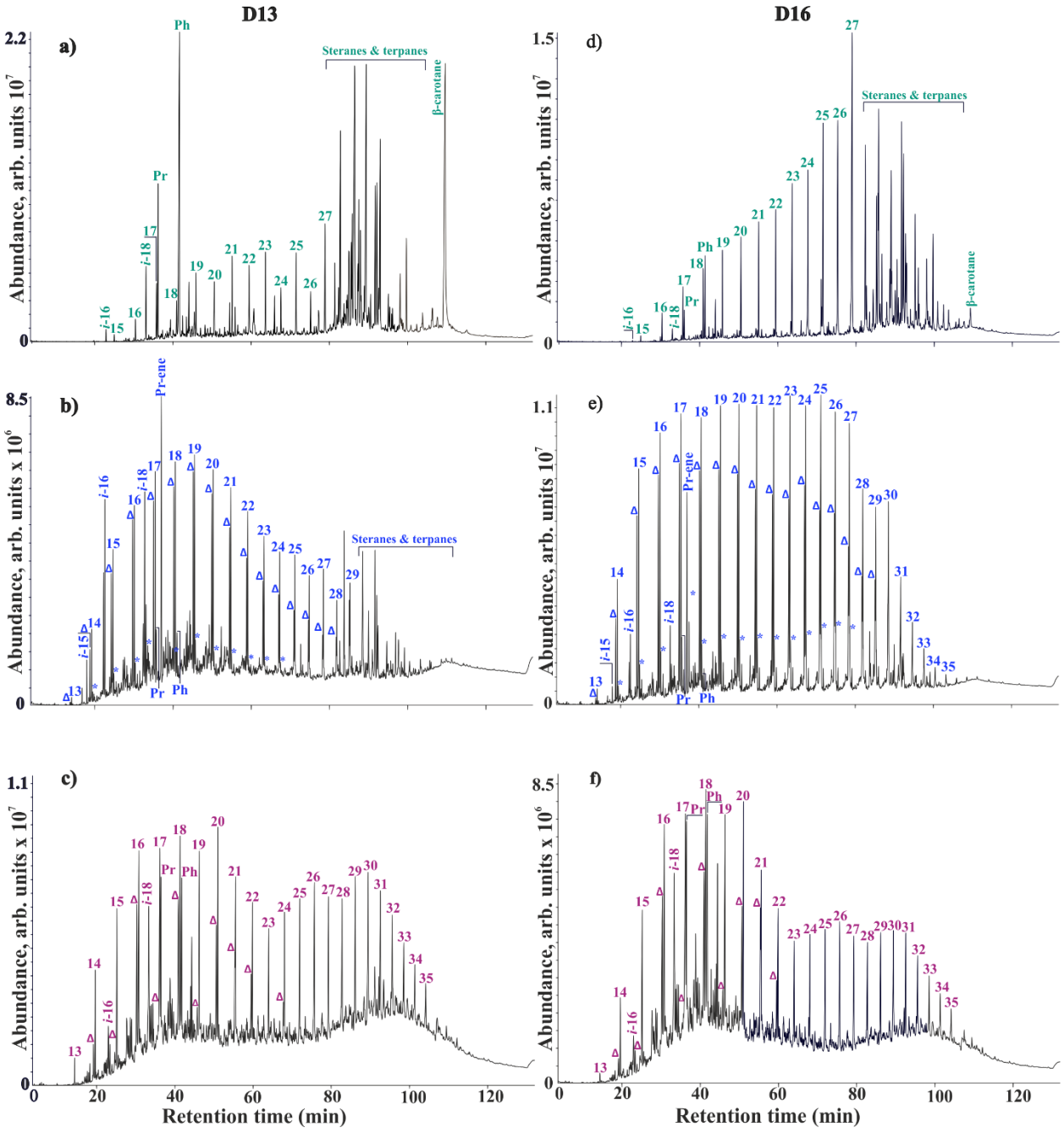

Fig. 1. Total Ion Chromatograms (TICs) of aliphatic fractions of initial bitumen of raw samples (a, d) and liquid pyrolysates from the open (b, e) and closed (c, f) system pyrolysis.

n-Alkanes are labelled according to their carbon number; Δ – terminal *n*-alkenes with the same number of carbon atoms as neighbor *n*-alkanes; * – non-terminal *n*-alkenes; Pr-ene – prist-1-ene; Pr – pristane; Ph – phytane; *i* – regular isoprenoids; arb. – arbitrary.

3.1.1. n-Alkanes

In initial bitumen, the identified *n*-alkanes ranged from C_{15} to C_{35}, with dominance of *n*-C_{27}, *n*-C_{29}, *n*-C_{31} homologues (Fig. 2a, d).

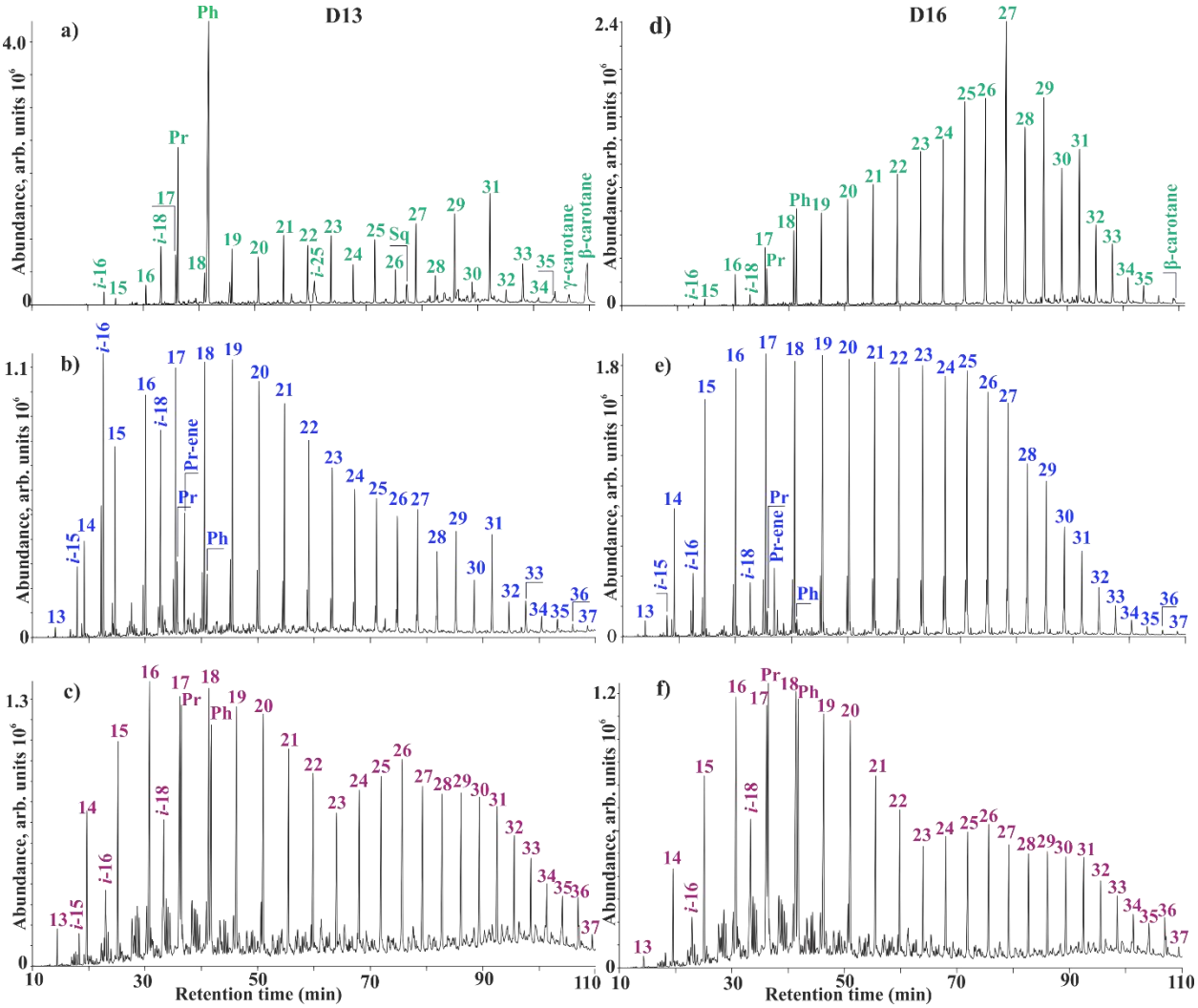

Fig. 2. GC-MS chromatograms of *n*-alkanes (*m/z* 71) in aliphatic fractions of initial bitumen (a, d) and liquid pyrolysates from the open (b, e) and closed (c, f) system pyrolysis.

Sq – squalane; for other abbreviations see the legend of Figure 1.

The distribution of *n*-alkanes in liquid pyrolysates differs from those in bitumen of raw samples. *n*-Alkanes are identified in almost the same range of C_{14}-C_{40} in all liquid pyrolysates (Fig. 2). The chromatograms reveal significant increase of *n*-alkanes abundance in relation to other hydrocarbons (Fig. 1) and the domination of lower homologues (Fig. 2). In addition to the fact

that the distribution of *n*-alkanes depends on maturity changes that particularly occur in the closed system pyrolysis, and lead to the shift of the *n*-alkane maximum toward lower homologues relative to initial bitumen, it also depends on the precursor material that is incorporated into the kerogen. The prevalence of lower homologues in liquid pyrolysates is consistent with the predominantly algal origin of OM (Table 1; van de Meent et al., 1980; Gajica et al., 2017a), although it was not clearly visible based on *n*-alkanes distribution in initial bitumen (Fig. 2a, d). Namely, as already has been mentioned, initial bitumen is characterized by the domination of higher homologues, which can be indicative of the contribution of both, higher land plants and algae, as well as their mixture in the precursor OM (Gelpi et al., 1968). It confirms that bounded biomarkers, early incorporated into the kerogen phase depicts source fingerprint of OM better than their counterparts in free bitumen.

The *n*-alkane distributions in all liquid pyrolysates are characterized by uniform abundances of odd and even homologues, resulting in a reduction of the CPI values (~ 1) in relation to the bitumen (Table 1). The main difference in the distribution of *n*-alkanes in pyrolysis products is a greater abundance of the higher homologues in liquid pyrolysate of the sample D13 from the CS relative to those obtained in the OS, whereas for the sample D16 the opposite trend is observed (Fig. 2b, c, e, f). This can be attributed to various microalgal origins (Gelpi et al., 1968), consistent with kerogen types and differences in TICs (Section 2.1; Fig. 1a, d), such as contribution of unicellular microalga *Botryococcus braunii* (Sinninghe Damsté et al., 1993), which presence has been already reported in Aleksinac oil shales (Ercegovac et al., 2003). Additionally, it can be caused by the longer exposure to thermal stress and pressure, as well as contact with native minerals (present in samples) in the CS, which contribute to more intense cracking of kerogen and to the defunctionalisation of molecules such as fatty acids, alcohols, thiols, ketones and esters that led to formation of free radicals during pyrolysis (Pakdel et al., 1999). These free radicals could be deactivated by hydrocarbons themselves, by hydrogen trapping, or by recombination, giving as the final products corresponding *n*-alkanes (Monthioux et al., 1985). In addition, in the CS, *n*-alkanes can also be formed by secondary reactions due to thermal cracking of heavy molecules such as substituted aromatic compounds (e.g. alkylbenzenes containing long alkyl chain), polar compounds, asphaltenes, cyclic compounds, as well as *n*-alkanes themselves (Franco et al., 2010).

3.1.2. n-Alkenes

Generally, *n*-alkenes do not occur or are present in low amounts in initial bitumen formed under natural conditions due to their low diagenetic stability, while artificial maturation of kerogen results in the occurrence of alkenes in liquid pyrolysates. Terminal *n*-alkenes are identified as pairs with the corresponding *n*-alkanes in liquid pyrolysates, ranging from C_{14} to C_{29} in the OS and from C_{14} to C_{24} in the CS (Fig. 1b, c, e, f). The prevalence of terminal *n*-alkenes, showing decreasing abundance with the increase of molecular weight, is common in pyrolysis products (Leif and Simoneit, 2000). *n*-Alkenes arise as intermediates during the thermal decomposition of long chain *n*-alkyl fragments of kerogen by the free radical mechanism. *n*-Alk-1-enes can also be formed by the β-elimination reactions of esters and amides by the loss of hydrogen atoms from primary alkyl-radicals or by the disproportionation of secondary alkyl-radicals (Ingram et al., 1983).

A greater abundance of *n*-alk-1-enes is detected in liquid pyrolysates from the OS, resulting in higher values of the Σ*n*-alk-1-enes/Σ*n*-alkanes ratio than in the liquid products from the CS (Table 1). This result was expected due to the short retention of degradation products in reaction medium of the open system, whereas in the closed system alkenes spent more time in contact with gases and catalysts from native minerals, which leads to their transformation.

The prevalence of linear hydrocarbons, represented by series of *n*-alkenes and *n*-alkanes, in TICs of aliphatic fractions of all liquid pyrolysates is characteristic of shale oils derived from lacustrine algal immature kerogen (Fig. 1b, c, e, f; Grice et al., 2003; Zhang et al., 2016). This HCs distribution in liquid pyrolysates may originate from algaenan. Algaenan is a highly aliphatic biopolymer which originates from cell wall remains of microalgae such as chlorophyta, eustigmatophyta and dinoflagellates (Douglas et al., 1990; Zhang et al., 2016). It is also known that the green microalgae *Botryococcus braunii* synthesizes long chain polymethylenic algaenan (Stasiuk, 1993; Derenne et al., 1994; Volkman, 2014). This biopolymer is present in a low content in algal OM, but it can be preserved and incorporated into kerogen due to its resistance to microbial and diagenetic breakdown (Gelin et al., 1997; Zhang et al., 2016; Zhang and Volkman, 2017). Therefore, algaenan can be a source of long chain alkyl-groups (particularly in sample D13, which contain mainly kerogen type I and has the quite high hydrocarbon generation potential; Section 2.1).

Table 1. The values of biomarker parameters

Sample	CPI (C_{15}-C_{35})	Pr/Ph	Pr/*n*-C_{17}	Ph/*n*-C_{18}	Σ*n*-alk-1-enes/ Σ*n*-alkanes	%C_{27} ααα(R)	%C_{28} ααα(R)	%C_{29} ααα(R)	C_{29} ααα 20S/(20S+20R)	ΣC$_{27}$-C$_{29}$ βαα(R)/ ΣC$_{27}$-C$_{29}$ ααα(R)	C_{29}αββ/(αββ+ααα)	Rc (%)	C_{31} αβ 22S/(22S+22R)	C_{30}βα/C_{30}αβ	GI	S/H
D13B	1.87	0.32	4.02	16.99	/	20.07	42.29	37.65	0.14	0.19	/	0.41	0.11	1.93	1.09	5.29
D16B	1.37	0.36	0.68	1.42	/	32.74	20.80	46.47	0.07	0.26	/	0.36	0.12	0.43	1.78	0.50
D13OS	1.13	1.23	0.33	0.25	0.83	25.96	45.60	28.44	0.18	0.63	/	0.44	0.30	4.25	4.37	0.33
D16OS	1.08	1.74	0.09	0.05	0.73	36.83	24.08	39.09	0.12	0.35	/	0.39	0.23	2.27	1.82	0.07
D13CS	1.03	1.03	0.93	0.84	0.53	30.20	33.62	36.18	0.47	/	0.50	0.76	0.55	0.74	1.07	0.31
D16CS	1.06	1.06	0.84	0.84	0.53	34.60	30.22	35.18	0.55	/	0.57	0.92	0.54	0.27	0.97	0.26
E.V.									0.52 - 0.55		0.67 - 0.71	/	0.57 - 0.62	≤ 0.15*		

B – Initial bitumen, extracted from raw oil shale samples; OS – open system pyrolysis; CS – closed system pyrolysis; CPI – Carbon Preference Index, CPI (C_{15}-C_{35}) = ½ x [Σodd(*n*-C_{15}-*n*-C_{35})/Σeven(*n*-C_{14}-*n*-C_{34}) + Σodd(*n*-C_{15}-*n*-C_{35})/Σeven(*n*-C_{16}-*n*-C_{36})]; Pr/Ph = Pristane/Phytane; %C_{27} ααα(R) – C_{27}/(C_{27} + C_{28} + C_{29}) of 5α(H)14α(H)17α(H)20R-steranes; %C_{28} ααα(R) – C_{28}/(C_{27} + C_{28} + C_{29}) of 5α(H)14α(H)17α(H)20R-steranes; %C_{29} ααα(R) – C_{29}/(C_{27} + C_{28} + C_{29}) of 5α(H)14α(H)17α(H)20R-steranes; C_{29}ααα 20S/(20S+20R) = C_{29} 5α(H)14α(H)17α(H)20S-sterane/C_{29} 5α(H)14α(H)17α(H)(20S+20R)-steranes; ΣC$_{27}$-C$_{29}$ βαα(R)/ΣC$_{27}$-C$_{29}$ ααα(R) = sum (C_{27}-C_{29}) 5β(H)14α(H)17α(H)20R-steranes/sum (C_{27}-C_{29}) 5α(H)14α(H)17α(H)20R-steranes; C_{29} αββ/(αββ + ααα) = C_{29} 5α(H)14β(H)17β(H)20R-sterane/(C_{29} 5α(H)14β(H)17β(H)20R + C_{29} 5α(H)14α(H)17α(H)20R)-steranes; Rc – calculated vitrinite reflectance = 0.49 x C_{29}ααα 20S/20R sterane + 0.33; C_{31}αβ 22S/(22S+22R) = C_{31} 17α(H)21β(H)22(S) homohopane/C_{31} 17α(H)21β(H)(22S+22R)-homohopanes; C_{30}βα/C_{30}αβ = C_{30}17β(H)21α(H)-moretane/C_{30}17α(H)21β(H)-hopane; GI – Gammacerane index, GI = (gammacerane × 10)/(gammacerane + C_{30}17α(H)21β(H)-hopane); S/H = [Σ(C_{27}-C_{29}) 5α(H)14α(H)17α(H)(20S+20R) + 5α(H)14β(H)17β(H)(20S+20R)-steranes]/[Σ(C_{29}-C_{33}) 17α(H)21β(H)-hopanes]; E.V. – equilibrium values (Peters et al., 2005); * – for Tertiary age.

3.1.3. Isoprenoid alkanes

In initial bitumen of both samples, pristane and phytane are the major regular isoprenoid alkanes (Fig. 1a, d). Regular isoprenoid alkanes C_{16} and C_{18} are also identified in both samples, while regular C_{25} isoprenoid is present in a low abundance in the sample D13 only. From the non-regular isoprenoids, β-carotane is present in both samples, but in the D16 sample in a low abundance, whereas C_{30} (squalane) and γ-carotane are identified in the sample D13 only.

More significant differences were observed in the distributions of isoprenoid alkanes between liquid products from two different pyrolytic systems, than between bitumen of initial samples. In the OS regular isoprenoid alkanes C_{16} and C_{18} are more abundant than pristane and phytane in both samples, whereas in the CS it is the opposite (Fig. 2b, c, e, f). Relatively high abundance of

regular isoprenoids (C_{15}, C_{16}, C_{18}) in liquid pyrolysates, particularly from the OS, could be attributed to isoprenoid precursors that are weakly bounded to kerogen and can be easily liberated by slight thermal treatment (Figs. 1 and 2 b, e; Brassell et al., 1986). The presence of C_{16} and C_{18} isoprenoids is consistent with algal origin of OM and they can be generated by pyrolysis of *Botryococcus braunii* (Derenne et al., 1994; Volkman, 2014). Pristane and phytane are mainly formed from chlorophyll pigments found in photosynthetic organisms (Volkman, 1986; Ishiwatari and Ishiwatari, 2004). In liquid pyrolysates from the OS, prist-1-ene is identified. This compound is typical product of thermal decomposition of immature kerogen (Höld et al., 2001). Namely, isoprenoid precursors such as chlorophyll or tocopherol generate pristane during geological maturation and prist-1-ene by thermal degradation during pyrolysis (Goossens et al., 1984; Zhang et al., 2016). Prist-1-ene does not appear in liquid pyrolysates from the CS probably due to prolonged exposure to thermal stress which caused its further transformation (Zhang et al., 2016). This is consistent with lower abundance of *n*-alk-1-enes in CS than in OS. Regular C_{25} isoprenoid and squalane (present in initial bitumen of the sample D13), as well as β- and γ-carotane are not identified in liquid pyrolysates. Interestingly, the same results were obtained by pyrolysis of the organic-rich sediments (using the same closed system and pyrolytic conditions) from the Valjevo-Mionica and Kremna basins (Stojanović et al., 2010; Perunović et al., 2014). The absence of these isoprenoids in liquid pyrolysates can be due to the sensitivity of their skeleton to thermal stress.

In initial bitumen of both raw samples, the uniform Pr/Ph ratio < 0.4 indicates sedimentation under reducing depositional conditions, which enhanced the preservation of algal-rich OM (Table 1; Gajica et al., 2017a). The values of Pr/Ph ratio are higher in all liquid pyrolysates than in initial bitumen (Table 1). In liquid products from the OS the Pr/Ph is > 1. That might be explained by a preferred release of pristane than phytane from isoprenoid moieties during thermal treatment of kerogen (Larter et al., 1979; Kissin, 1993). In liquid pyrolysates from the CS the Pr/Ph ratio is ~ 1 (Table 1). This might be caused by the increase in maturity (Connan, 1974; Peters et al., 2005) or by the fact that both isoprenoid alkanes are formed at the same rate during artificial maturation (Stojanović et al., 2010). As expected, the Pr/*n*-C_{17} and Ph/*n*-C_{18} ratios decrease during the thermal treatment of kerogen (Table 1).

3.1.4. Ketones

In initial bitumen, the *n*-alkan-2-ones are identified in the range of C_{12}-C_{33}, with uniform distribution of even and odd homologues in the sample D13 and dominance of odd homologues with maximum at C_{27} in the sample D16 (Fig. 3a, d). It is noteworthy that distribution of ketones is very similar to those of *n*-alkanes, confirming their common origin (Figs. 2, 3a, d). In addition to *n*-alkan-2-ones, a C_{18} isoprenoid ketone (6,10,14-trimethylpentadecan-2-one) was identified in initial bitumen of both raw samples, as the most prominent compound.

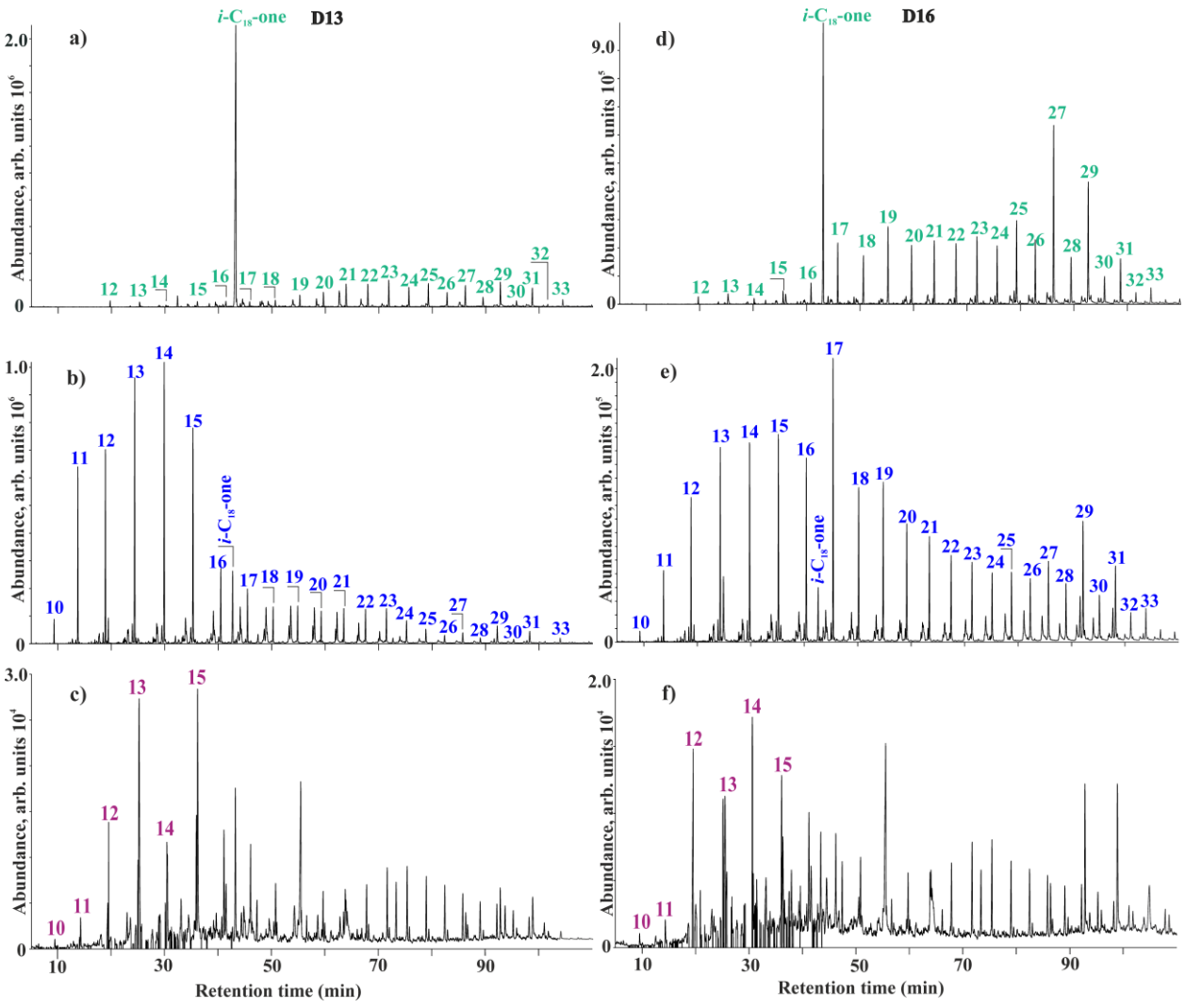

Fig. 3. GC-MS chromatograms of *n*-alkan-2-ones (*m/z* 58) in initial bitumen (a, d) and liquid pyrolysates from the open (b, e) and closed (c, f) system pyrolysis.

n-Alkan-2-ones are labelled according to their carbon number; *i*-C_{18}-one – C_{18} regular isoprenoid ketone (6,10,14-trimethylpentadecan-2-one); arb. – arbitrary.

n-Alkan-2-ones are also present in liquid pyrolysates. They are identified in the range C_{10}-C_{33} in liquid products from the OS; whereas in the CS the distribution starts from C_{10}, but due to the low abundance and co-elution of the other compounds precise determination of higher homologues (>C_{15}) was impossible (Fig. 3). In comparison to bitumen, both liquid pyrolysates from the OS are characterized by prevalence of lower *n*-alkan-2-ones and more uniform distribution of even and odd homologues, as well as significantly lower abundance of C_{18} isoprenoid ketone. The results are in accordance with changes in *n*-alkane and isopreniod distributions (decrease of CPI, Pr/*n*-C_{17} and Ph/*n*-C_{18} in the OS liquid products in comparison to initial bitumen; Table 1). In liquid pyrolysates from the CS lower homologues notably prevail, while C_{18} isoprenoid ketone is absent.

n-Alkan-2-ones have been found in marine and lacustrine sediments (Volkman et al., 1983; Cranwell et al., 1987). β-Oxidation of fatty acids, followed by decarboxylation, and β-oxidation of corresponding *n*-alkanes are reported as the main biological formation pathways of *n*-alkan-2-ones in sedimentary OM (Volkman et al, 1983; Cranwell, et al., 1987). Predominance of odd over even homologues is characteristic of microbiological origin (Brassell et al., 1980; Tuo and Li, 2005), while maximum at C_{27} can indicate origin from microalgae, phytoplankton and higher plants (Ying and Fan, 1993; González-Vila et al., 2003). The C_{18} isoprenoid ketone is found in many recent sediments (Rontani and Volkman, 2003). It can be formed by photosensitized oxidation of some isoprenoid alkanes, such as pristane and phytane (Rontani and Giral, 1990), bacterial degradation of phytol (Rontani and Giral, 1990), photodegradation of chlorophyll-*a* (Rontani et al., 1991), and by alkaline hydrolysis of tocopherols (Rontani and Volkman, 2003).

It is known that the *n*-alkane-2-ones and C_{18} isoprenoid ketone occur in shale oils (Šaban et al., 1980; Rovere et al., 1983; Sinninghe Damsté et al., 1993). They can be attributed to the algaenan from different types of algae (Zhang et al., 2016; Zhang and Volkman, 2017; Zhang et al., 2021). In some studies, these ketone compounds were associated with the Botryococcus *braunii* (Dubreuil et al., 1989; Gelin et al., 1993; Derenne et al., 1994). They can arise by thermal degradation of kerogen by breaking β-keto groups that are bounded to kerogen (Rovere et al., 1983). The cleavage of this structure leads to the appearance of *n*-alkane-2-ones, as well as the increase of the Σalkenes/Σalkanes ratio (Zhang and Volkman, 2017). The domination of lower homologues in all liquid pyrolysates can be a result of thermal treatment. Significantly lower abundance of C_{18} isoprenoid ketone in liquid products from the OS and absence of this

compound in liquid pyrolysates from the CS can be explained by sensitivity of its structure to thermal stress. Namely, Zhang et al. (2016) reported that C_{18} isoprenoid ketone was identified only at temperature 310 ºC during stepwise pyrolysis at temperatures from 310 to 660 ºC.

3.1.5. Fatty acid methyl esters

In initial bitumen of raw samples, the fatty acid methyl esters are identified in the range of C_{13}-C_{33} (Fig. 4a, d). The lower homologues with maximum at C_{17} are dominant in the sample D13, while in the sample D16, consistent with distributions of *n*-alkanes and *n*-alkan-2-ones, higher homologues prevail, with maximum at C_{29}.

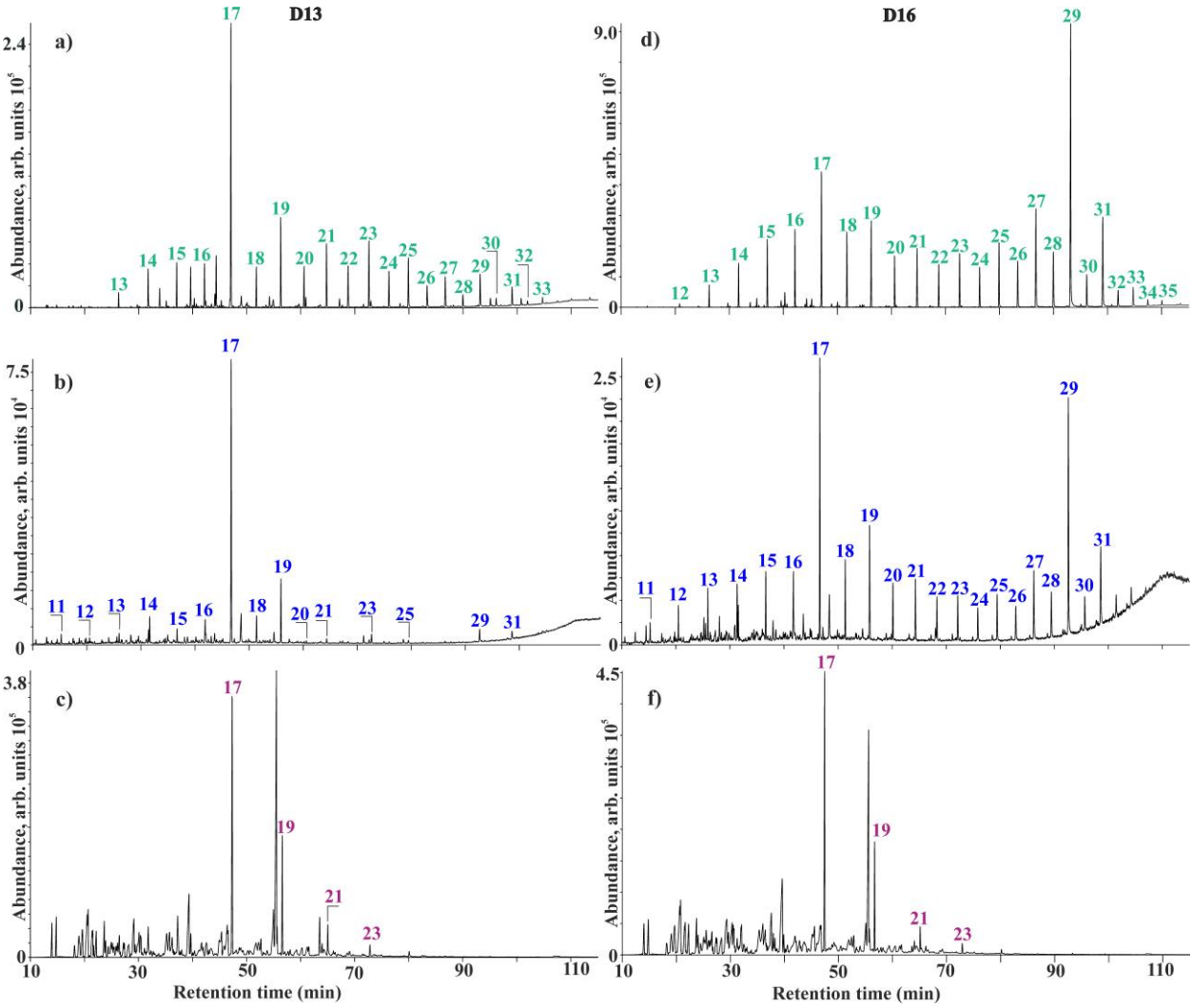

Fig. 4. GC-MS chromatograms of fatty acid methyl esters (*m/z* 74) in initial bitumen (a, d) and liquid pyrolysates from the open (b, e) and closed (c, f) system pyrolysis.

Fatty acid methyl esters are labelled according to their total carbon number; arb. – arbitrary.

Carboxylic acids methyl esters occur widely in natural products and it is known that lacustrine sediments usually contain them (Cranwell, 1984). The lower homologues of fatty acid methyl esters (< C_{20}) are characteristic of aquatic organisms (Cranwell, 1984) and many algae and bacteria (Merritt et al., 1991), while higher homologues indicate terrestrial plants as precursors of OM (Pakdel et al., 1999). The very scarce distribution of fatty acid methyl esters in the CS pyrolysis could be explained by β-elimination reactions of esters into *n*-alk-1-enes that are mainly completed before the catagenetic stage (Alexander et al., 1992; Zhang et al., 2021).

3.1.6. Steranes

In initial bitumen of raw samples, the distributions of steranes show domination of regular C_{27}-C_{29} steranes with ααα(R) configuration. Steranes with βαα(R)-configuration, typical for immature diagenetic OM, are identified in the C_{27}-C_{29} range, while ααα(S) steranes are represented by C_{29} homologue only. Lower molecular weight, C_{21}-C_{26} steranes are present in a low abundance in both samples, whereas C_{28}-C_{30} 4-methylsteranes are identified in the sample D16 (Fig. 5a, d).

The distributions of steranes in liquid pyrolysates from the OS are very similar with those in bitumen extracts of raw samples, and even show higher amount of βαα(R)-isomers (Fig. 5a, b, d, e). The result clearly indicates well protection of biogenic stereochemistry in kerogen bounded steranes and its preservation during the OS pyrolysis. On the other hand, pyrolytic experiments in the CS, lead to significant differences in the distribution of steranes in relation to their distribution in liquid products from the OS and bitumen (Fig. 5). In the CS liquid pyrolysates, beside C_{27}-C_{29} regular ααα(R) steranes, C_{27}-C_{29} homologues with thermodynamically more stable configurations, ααα(S), αββ(S) and αββ(R), as well as, βα- and αβ-diasteranes are also present. Thermodynamically unstable steranes with βαα(R)-configuration and C_{28}-C_{30} 4-methylsteranes (identified in the sample D16) were absent (Fig. 5c, f). This indicates that isomerisation occurs to a major extent during the release and defunctionalisation of bounded steroids and hopanoids and further facilitates in free biomarkers with the increasing of time spent under the thermal treatment (secondary processes; Murray et al., 1998).

The distribution of C_{27}-C_{29} regular ααα(R) steranes in liquid products from both type of pyrolytic systems has almost the same trend as in bitumen of raw samples, $C_{28} > C_{29} > C_{27}$ in the sample

D13 and $C_{29} > C_{27} > C_{28}$ in the sample D16 (Fig. 5, Table 1). However, particularly in liquid pyrolysates from the CS, an equalization of the relative abundances of regular C_{27}-C_{29} steranes is apparent, indicating the loss of the fingerprint from the biological precursors. The result can be attributed to secondary reactions enabled in the CS, and it is consistent with observations reported in previous studies (e.g. Lu and Kaplan, 1992; Vuković et al., 2016). On the other hand, it was observed that the amount of steroid side chain cleavage occurring during hydropyrolysis is low (Love et al., 2005). Another explanation for the enrichment of the CS pyrolysis products in C_{27} steranes is the early incorporation of algal derived biomarkers (e.g. C_{27} steranes) into the kerogen phase during kerogen formation, whilst the free bitumen contains greater amount of higher plant C_{29} steranes, originating from the lake catchment, in comparison to kerogen (Love et al., 1998; Bowden et al., 2006). This is in line with greater increase of content of C_{27} steranes in the CS pyrolysate of the sample D13 (enriched in algal OM) than in the sample D16, in relation to initial bitumen (Table 1). At higher maturities (catagenesis), high quantity of released kerogen bound steranes would enrich the free bitumen in C_{27} steranes, consistent with the known increase in the proportion of C_{27} steranes with increase of thermal maturity (Peters et al., 2005).

4-Methylsteranes C_{28}-C_{30}, present in sample D16, are identified in corresponding OS liquid pyrolysates, and have the same trend $C_{30} \approx C_{28} > C_{29}$ as in bitumen (Fig. 5d, e). They are indicative of prymnesiophyta, certain bacteria, diatoms, dinoflagellates and aquatic macrophytes in lacustrine or marine environments (Wolff et al., 1986; Klink et al., 1992; Peters et al., 2005). 4-Methylsteranes are not identified in CS liquid pyrolysate (Fig. 5f), confirming certain loss of the source fingerprint in the CS. Their absence could be attributed to demethylation reactions.

Low molecular weight steranes C_{21}-C_{26} are identified in a greater abundance in liquid products from both type of pyrolysis than in bitumen (Fig. 5), which can indicate the increase in maturity of OM (Wingert and Pomerantz, 1986). Furthermore, according Li and Jiang (2001), and Lu et al. (2009) their generation during late diagenesis indicates that the precursors of C_{21}-C_{25} steranes are associated with microbially mediated diagenetic processes in the specific depositional environment. Although, diatoms are generally considered as the principal precursors of C_{26} 24-norcholestanes (Holba et al., 1998; Peters et al., 2005), the impact of dinoflagellates cannot be rule out, since Wang et al. (1996) detected C_{26} 24-norcholestane among the hydrous pyrolysis products of dinoflagellates; Rampen et al. (2007) identified 24-norsterols in dinoflagellate *Gymnodiniium simplex*, and Wang et al. (2008) confirmed that C_{26} 24-norcholestanes in Eocene–

Oligocene lacustrine sediments from the Jiyang sub-basin (Bohai Bay Basin, eastern China) originated from dinoflagellates.

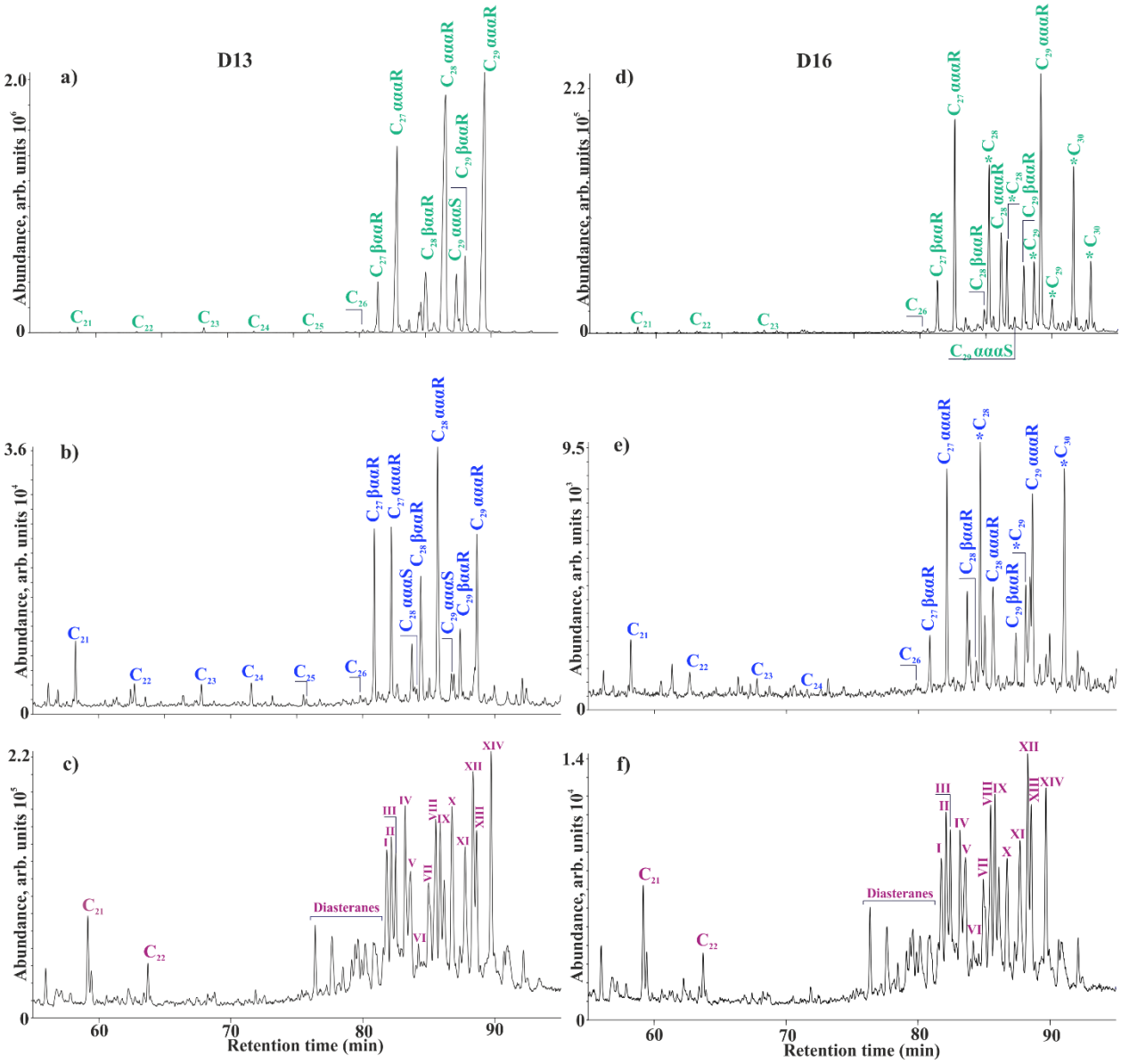

Fig. 5. GC-MS chromatograms of steranes (*m/z* 217) in initial bitumen (a, d) and liquid pyrolysates from the open (b, e) and closed (c, f) system pyrolysis.

C_{21}-C_{26} steranes with 14α(H)17α(H) configuration; βαα and ααα designate 5β(H)14α(H)17α(H) and 5α(H)14α(H)17α(H) configurations in steranes; S and R designate configuration at C-20 in steranes; *C_{28}-C_{30} – C_{28}-C_{30} 4-methylsteranes; I – C_{27} 5α(H)14α(H)17α(H)20(S)-sterane + C_{28} 13α(H)17β(H)20(S)-diasterane; II – C_{27} 5α(H)14β(H)17β(H)20(R)-sterane + C_{29} 13β(H)17α(H)20(S)-diasterane; III – C_{27} 5α(H)14β(H)17β(H)20(S)-sterane + C_{28} 13α(H)17β(H)20(R)-diasterane; IV – C_{27} 5α(H)14α(H)17α(H)20(R)-sterane; V – C_{29} 13β(H)17α(H)20(R)-diasterane; VI – C_{28} 5α(H)14α(H)17α(H)20(S)-sterane; VII – C_{29} 13α(H)17β(H)20(S)-diasterane; VIII – C_{28} 5α(H)14β(H)17β(H)20(R)-sterane + C_{29} 13α(H)17β(H)20(R)-diasterane; IX – C_{28} 5α(H)14β(H)17β(H)20(S)-

sterane; X – C_{28} 5α(H)14α(H)17α(H)20(R)-sterane; XI – C_{29} 5α(H)14α(H)17α(H)20(S)-sterane; XII – C_{29} 5α(H)14β(H)17β(H)20(R)-sterane; XIII – C_{29} 5α(H)14β(H)17β(H)20(S)-sterane; XIV – C_{29} 5α(H)14α(H)17α(H)20(R)-sterane; arb. – arbitrary.

The values of sterane maturation parameter C_{29} ααα 20S/(20S+20R) in liquid pyrolysates from the OS are insignificantly higher than in bitumen (Table 1), suggesting almost equal maturity of the initial bitumen and OS pyrolysis product. On the other hand, the value of the sum (C_{27}-C_{29}) βαα(20R)/sum (C_{27}-C_{29}) ααα(20R) steranes ratio is very close in initial bitumen and the OS pyrolysis product of the sample D16, containing mixed type I/II kerogen, whereas the sample D13, containing type I kerogen (enriched in algal OM, representing the main source of steranes) exhibited notably higher value of this parameter in the pyrolysate from the OS than in initial bitumen (Table 1). The increase of content of βαα(20R) steranes in the sample D13 is particularly apparent for C_{27} homologue (Fig. 5a, b), which is generally typical algal biomarker fingerprint. This confirms an assumption derived from *n*-alkane distributions that the OS pyrolysate can provide even clearer data about the sources of OM, than initial bitumen. In addition, the preservation of biological stereochemistry 5β(H)14α(H)17α(H)(20R) in steranes released by the OS pyrolysis confirms conclusions from previous studies (Rubinstein et al., 1979; Russell et al., 2004; Lockhart et al., 2008; Wu et al., 2013) that bounded biomarkers retain their native structure better than free biomarkers present in bitumen, as well as that stereochemistry of former is not altered by the OS pyrolysis that is in line with results of Love et al. (1995, 1997) and Bishop et al. (1998). Therefore, the applied type of the OS pyrolysis to certain extent is comparable with catalytic hydropyrolysis (HyPy), which utilizes a dispersed sulfide molybdenum catalyst and high hydrogen pressures (>10 MPa) to ensure minimal structural rearrangement of the released biomarkers (Love et al., 1995, 1997; Murray et al., 1998, Meredith et al., 2008) and recently modified the microscale sealed vessel (MSSV) pyrolysis (Wu and Horsfield, 2019).

In liquid pyrolysates from the CS, the values of the C_{29} ααα 20S/(20S+20R) ratio are in the equilibrium range (D16) or near the equilibrium range (D13; Table 1). The maturation parameter C_{29} αββ/(αββ+ααα) is calculated for liquid pyrolysates from the CS, only, because in other samples αββ steranes are absent. The values of this parameter are slightly lower than proposed equilibrium values (Table 1). The reason can be extremely slow process of the sterane isomerization reaction ααα → αββ, that needs an appropriate period of time, in addition to the

thermal stress. Based on the sterane maturity ratios it can be estimated that by CS early to main "oil window" phase was reached (corresponding to vitrinite reflectance of 0.76-0.92 %; Table 1).

3.1.7. Terpanes

In initial bitumen of raw samples, the terpane distribution is characterized by a relatively low abundance of tricyclic and tetracyclic terpanes and domination of pentacyclic terpanes (hopanes). In the hopane distribution C_{27} 17β(H)- and 17α(H)-trisnorhopane, C_{29}-C_{32} βα moretanes, C_{29}-C_{32} αβ hopanes and C_{29}-C_{33} ββ hopanes are present. Gammacerane is identified in both samples (Fig. 6a, d).

The distribution of terpanes in liquid products from both pyrolytic systems is characterized by the domination of pentacyclic hopanes (βα and αβ), and the presence of tricyclic and tetracyclic terpanes in low amounts, as in the bitumen of raw samples. In addition, C_{31}-C_{35} homohopanes are identified in all liquid pyrolysates, while in the bitumen of raw samples only C_{31}-C_{32} homologues are present in traces (Fig. 6). This is in line with conclusions of Farrimond et al. (2003) that significant amount of hopanes is present in kerogen bounded form in immature samples.

The distributions of hopanes in liquid products from the OS (consistent with sterane distributions) show immature pattern. Hopanoid fingerprints are characterized by the high abundance of thermodynamically unstable diagenetic isomers with ββ-configuration and the presence of hopenes, especially C_{27}-hop17(21)-ene (Fig. 6b, e), confirming well protection of biological structure in bounded kerogen phase and its preservation by the OS pyrolysis. On the other hand, liquid products from the CS displayed notably more mature hopane distributions, which are characterized by presence of neohopanes (C_{27}Ts, C_{29}Ts), the prevalence of thermodynamically more stable αβ- over βα- isomers, and dominance of 22S- relative to less stable 22R epimers in the C_{31}-C_{35} homohopane series, confirming significant biomarker isomerisation in the CS. Gammacerane is identified in all liquid pyrolysates in relatively low abundance, as in initial bitumen.

Prokaryotes are considered as the main biological precursors of hopanes (Ourisson et al., 1979). The main precursor of gammacerane is the membrane lipid tetrahymanol, which can be found in ciliates, ferns, an anaerobic rumen fungus and photosynthetic bacteria in stratified water columns (Peters et al., 2005; Sugden et al., 2005). The value of gammacerane index (GI) in initial bitumen

is higher in the raw sample D16 than D13, while in liquid pyrolysates it is opposite, being more pronounced in the OS (Table 1).

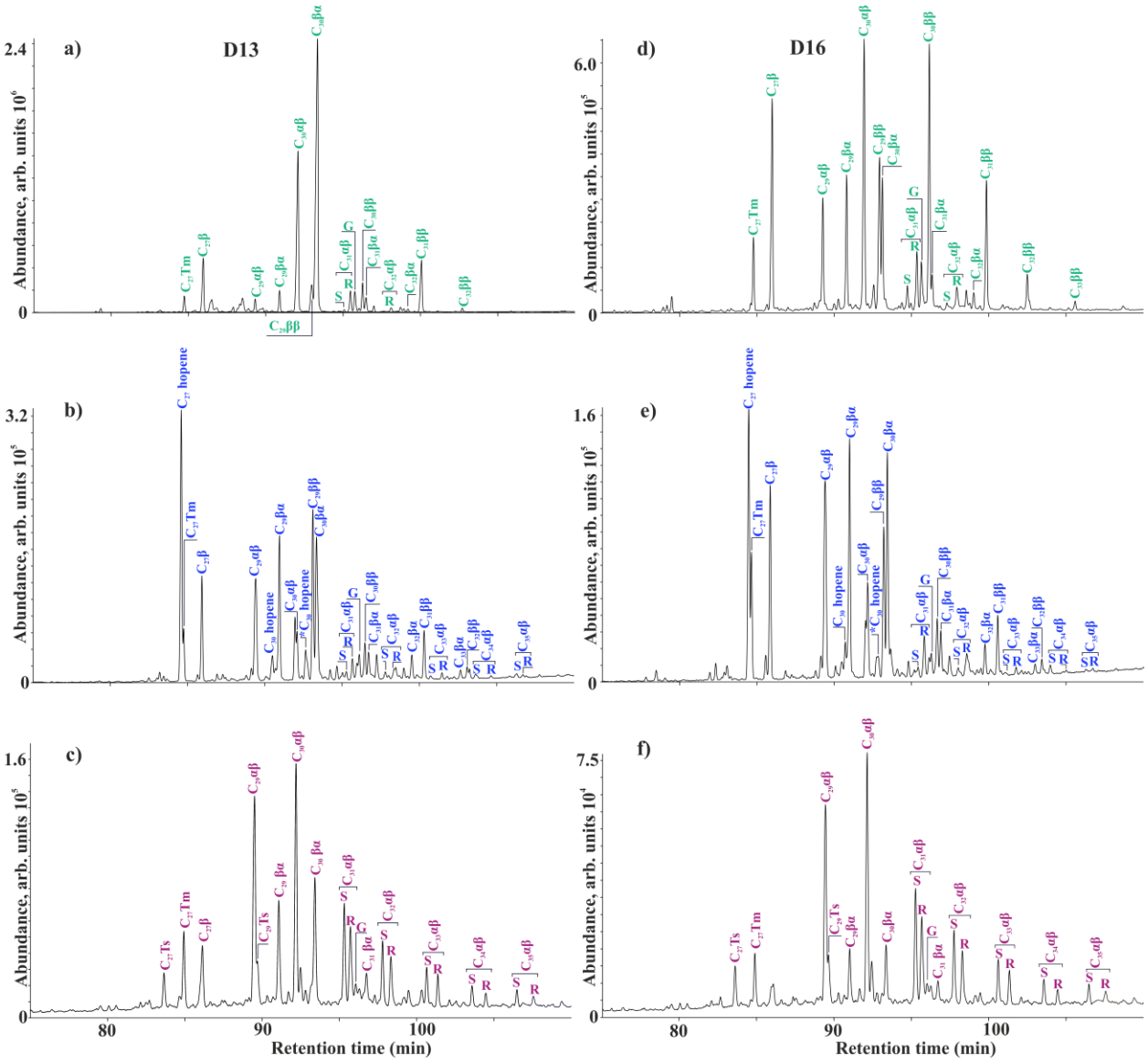

Fig. 6. GC-MS chromatograms of terpanes (*m/z* 191) in initial bitumen (a, d) and liquid pyrolysates from the open (b, e) and closed (c, f) system pyrolysis.

C_{27}Ts – C_{27} 18α(H)-22,29,30-trisnorneohopane; C_{27}Tm – C_{27} 17α(H)-22,29,30-trisnorhopane; C_{27}β – C_{27} 17β(H)-22,29,30-trisnorhopane; C_{29}Ts – C_{29} 18α(H)-30-norneohopane; C_{27} hopene – C_{27} trisnorhop-17(21)-ene; C_{30} hopene – C_{30} hop-17(21)-ene; *C_{30} hopene – C_{30} hop-13(18)-ene; αβ, βα and ββ designate configurations at C-17 and C-21 in C_{29}-C_{35} hopanes; S and R designate configuration at C-22 in C_{31}-C_{35} homohopanes; G – gammacerane; arb. – arbitrary.

Comparable to the initial bitumen, the liquid pyrolysate of the sample D16 from the OS has elevated content of C_{27} 17β(H)-trisnorhopane (Fig. 6d, e), which was obtained in high amount by flash pyrolysis of several families of alphaproteobacteria, betaproteobacteria and cyanobacteria (De Rosa et al., 1971). The C_{27}-C_{30} hopenes found in liquid pyrolysates from the OS are diagenetic products and may be generated from the same source as C_{27}-C_{35} hopanes, by breakdown or structural rearrangement of diploptene, diplopterol and bacteriohopanepolyols that synthesize certain types of bacteria and cyanobacteria (Rohmer et al., 1984; Sugden et al., 2005; Love et al., 2005). The steranes/hopanes ratio (S/H, Table 1) < 1 in the initial bitumen of raw sample D16 depicts higher input of prokaryotic organisms, while S/H > 1 in the bitumen of D13 sample is indicative for dominant algal input (Peters et al., 2005), consistent with kerogen type (Rock-Eval data; Gajica et al., 2017a). Decrease of the S/H ratio, observed in all liquid pyrolysates, in comparison to initial bitumen (particularly those from the OS; Table 1), implies that content of hopanes in the kerogen-bound biomarkers is higher than amount of steranes due to the fact that hopanes are generally bound into macromolecules via a larger number of binding sites than steranes (Hofmann et al., 1992; Bowden et al., 2006).

The hopane maturation parameter, C_{31}αβ 22S/(22S+22R) (Table 1) indicates a slightly elevated maturity in liquid products obtained from the OS than in initial bitumen, while this difference is remarkable in the liquid pyrolysates from the CS. On the other hand, the C_{30}βα/C_{30}αβ ratio is higher in the OS pyrolysates than in initial bitumen, and as expected apparently lower in the CS pyrolysates of both samples. The elevated values of the C_{30}βα/C_{30}αβ in liquid products (obtained by mild pyrolysis methods that generally preserving stereochemistry of kerogen bounded biomarkers unaltered) in relation to free bitumen were often reported in literature (Murray et al., 1998; Yoshioka and Ishiwatari, 2002; Bowden et al., 2006; Berwick et al., 2010). Enhanced abundance of C_{30}βα moretane in kerogen bounded fraction can be attributed to relatively low energy barrier for conversion of ββ hopane into more stable βα and αβ isomers that readily occurs during diagenesis in free, but also to some extent probably in bounded biomarkers (Seifert and Moldowan, 1980). Furthermore, the isomerisation ββ → βα and αβ can occur even prior to incorporation of hopanoid moieties into kerogen via covalent bonding, adsorption or occlusion, since βα moretane and αβ hopane are regularly present in very immature samples (e.g. lignites, having huminite reflectance of about 0.30 %Rr; Stojanović et al., 2012; Stojanović and Životić, 2013) On the other hand, energy barrier for conversion of βα moretane to αβ hopane is higher,

requires more intense thermal stress (Seifert and Moldowan, 1980) and occurs later mainly in free, rather than better protected bounded biomarkers. Since studied samples are immature, bounded hopanes are enriched in $C_{30}\beta\alpha$ moretane, comparing to free bitumen, and it was readily released (along with other immature hopanoid fingerprints such as, hopenes and ββ hopanes; Fig. 6b, e) during the OS pyrolysis, which does not alter stereochemistry, particularly in rings of bounded biomarkers.

Generally, the obtained values of hopane maturity ratios corroborate to the conclusion derived based on the sterane maturity indicators, suggesting late diagenetic phase for liquid pyrolysates from the OS and catagentic stage for liquid pyrolysates from the CS. Maturity parameters based on epimerisation R → S at the chiral C-atom (C-20 in steranes and C-22 in homohopanes) reached equilibrium values in the both liquid pyrolysates from the CS, in difference to C_{29} αββ/(αββ+ααα) and $C_{30}\beta\alpha/C_{30}\alpha\beta$ ratios which consider isomerization in the ring (Table 1). This result is in accordance with the fact that activation energy for the isomerization in the ring of polycylic biomarkers is higher than those required for epimerization at the chiral C-atom in their side chain (Peters et al., 2005). Furthermore, maturity changes in rings, in addition to thermal stress, require an appropriate period of time, which are usually insufficient by pyrolytic simulation of maturation (Peters et al., 2005; Stojanović et al., 2010; Vuković et al., 2016).

The sterane and hopane maturity ratios suggest that mixed type I/II kerogen (sample D16) attained slightly higher maturity level by the closed system pyrolysis than type I kerogen (sample D13). Partly, this can be attributed to higher content of sulfur in sample D16 (Section 2.1).. Namely, C-S and particularly, S-S bonds are weaker than C-C bonds, and consequently relatively easily cleavage at low thermal-stress levels, forming the initiating free radicals that allow the further thermal cracking of C-C bonds to occur at a faster rate and lower temperatures (Lewan, 1998). This is confirmed by very similar values of the C_{29} ααα20S/(20S+20R) and C_{31} αβ 22S/(22S+22R) ratios in the OS liquid products of samples D13 and D16, being slightly higher in former, because in the OS the initiating sulfur radicals are removed from the maturing OM by carrier gas and therefore unavailable to participate fully in initiating thermal cracking reactions (Reynolds et al., 1995). Conversely, the CS pyrolysis maintains initiating sulfur radicals in contact with thermally maturing kerogen, thus can contribute to higher values of biomarker maturity ratios in the CS liquid product of the sample D16 in comparison to D13, because in addition to sulfurization/desulfurization processes, high concentrations of sulfur radicals might

constrain the reactions from biological precursors or their intermediates into rearranged compounds (Wang et al., 2010). Elevated C_{29} ααα20S/(20S+20R) and C_{29}αββ/(αββ+ααα) sterane maturity parameters were occasionally observed in extracts of immature carbonate rocks and corresponding oils enriched in sulfur (ten Haven et al., 1986; Rullkötter and Marzi, 1988; Peters et al., 1990; Wang et al., 2010). Since, the D16 sample in addition to elevated sulfur content (6.11 wt. %), is characterized by prevalence of carbonates (63.87 wt. %) in mineral matter, whereas the D13 sample has notably lower amounts of sulfur and carbonates (0.21 wt. % and 33.95 wt. %, respectively; Gajica et al., 2017a), the observed differences in values of biomarker maturity ratios in their CS liquid products are quite reasonable and in accordance with findings from previous studies.

3.2. Compound specific isotope analysis of n-alkanes in initial bitumen and liquid pyrolysates

The results of compound specific carbon isotope analysis ($\delta^{13}C$) of *n*-alkanes in aliphatic fractions of initial bitumen and liquid pyrolysates from the open and closed systems are presented in Figure 7.

3.2.1. Initial bitumen of raw samples

The isotope $\delta^{13}C$ values of individual C_{15}-C_{25} *n*-alkanes range between –30.2 and –33.8 ‰ with average value of –31.9 ‰ in the sample D13 (measurement of $\delta^{13}C$ for homologues having more than 25 C-atoms was impossible due to the co-elution of steranes and hopanes; Fig. 1a). In the sample D16, the $\delta^{13}C$ values of individual C_{15}-C_{29} *n*-alkanes range from –28.7 to –32.5 ‰ (average value, –30.9 ‰). In the initial bitumen, hydrocarbons originate from free lipids, naturally generated in geological conditions during diagenetic processes and their $\delta^{13}C$ values mainly depend on source material and depositional environment. Generally, low $\delta^{13}C$ values of *n*-alkanes in initial bitumen of raw oil shale samples indicate depletion in the heavier isotope ^{13}C, which is more pronounced in the sample D13.

A relatively wide range of $\delta^{13}C$values of *n*-alkanes (difference up to 3.6 ‰) in the analyzed samples may result from diverse carbon sources (algae, bacteria and higher plants). The obtained low $\delta^{13}C$ values (< –28 ‰) could be also attributed to algal origin of the OM (Collister et al., 1994; Lichtfouse et al.1994; Love et al., 1998; Liu et al., 2015) that is consistent with Rock-Eval data (Section 2.1; Gajica et al., 2017a) and molecular composition of bitumen and liquid

pyrolysates from OS (Section 3.1). A slightly elevated values of $\delta^{13}C$ in the sample D16 in comparison to D13 can be attributed to higher contribution of prokaryotic organisms, confirmed by lower S/H ratio (Table 1) and different conditions in depositional environment (Gajica et al., 2017a). The sample D13 is characterized by more uniform $\delta^{13}C$ values than sample D16, in accordance with notably prevalent algal type I kerogen. Typical feature of the sample D16 is enrichment in ^{13}C of C_{22}-C_{26} *n*-alkanes, which is indicative for additional source of OM, since mid-chain *n*-alkanes, beside from algae, can be derived from bacteria or aquatic macrophytes (Neto et al., 1998; Ficken et al., 2000).

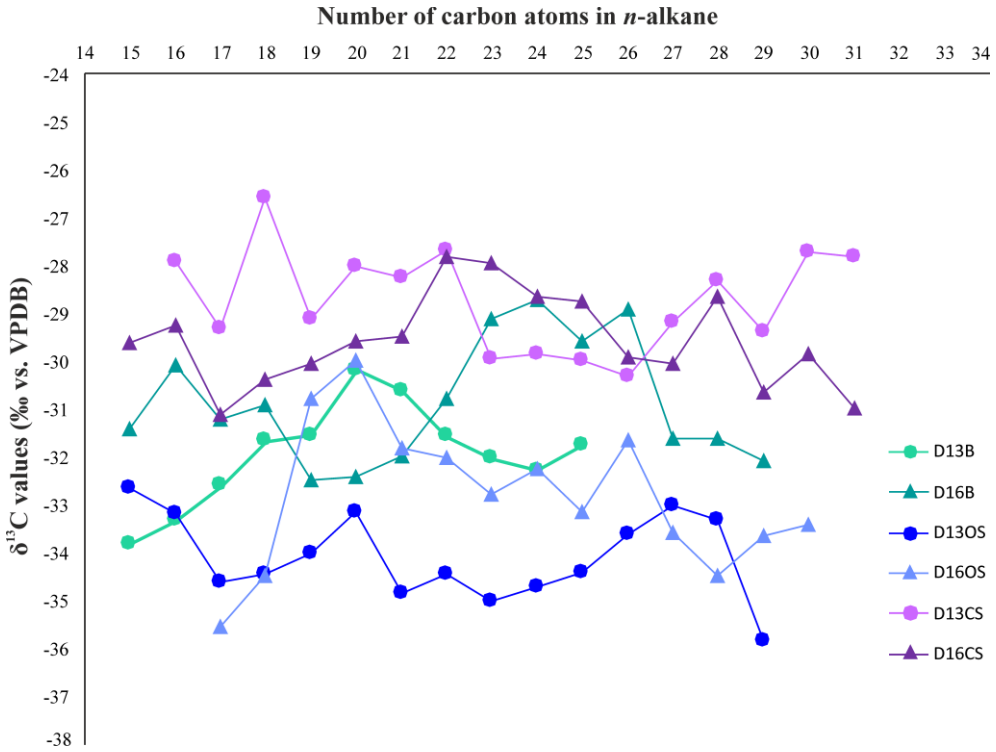

Fig. 7. $\delta^{13}C$ values of individual *n*-alkanes in initial bitumen and liquid pyrolysates from the open and closed system pyrolysis.

B – bitumen; OS – open system; CS – closed system.

3.2.2. Liquid pyrolysates

The $\delta^{13}C$ values of individual C_{15}-C_{29} *n*-alkanes in liquid pyrolysates from the OS of the sample D13 are between –32.6 and –35.8 ‰ (average value –34.1 ‰). In the OS liquid pyrolysate of the sample D16 the $\delta^{13}C$ values of individual C_{17}-C_{30} *n*-alkanes range from –30.0 to –33.7 ‰, average value, –32.8 ‰. In the liquid pyrolysates hydrocarbons are released from the kerogen

due to thermal decomposition and further alterations, and generally $\delta^{13}C$ values of individual *n*-alkanes increase with increasing maturity as a result of ^{13}C enrichment (Lewan, 1983; Tian et al., 2017). However, the average $\delta^{13}C$ values in liquid products from the OS show a decrease of ~ 2 ‰ in comparison to bitumen. This indicates that during thermal treatment of immature kerogen in OS, there is releasing of weakly bounded hydrocarbons, associated with preferential cleavage of $^{12}C–^{12}C$ bonds in aliphatic moieties weakly bounded to kerogen. Immediately after releasing, hydrocarbons leave the reaction medium, being carried by an inert gas, and collected in a cold trap that prevents secondary processes. As a result, *n*-alkanes in OS liquid pyrolysates are enriched in ^{12}C isotope in comparison to initial bitumen. Isotopically light individual *n*-alkanes are characteristic for immature kerogen (Schidlowski, 1986; Love et al., 1998) and were also found in oils from lacustrine environment (Bjorøy et al., 1991).

The $\delta^{13}C$ values of individual C_{16}-C_{31} *n*-alkanes in liquid pyrolysate from the CS of the sample D13 are between –26.6 and –30.3 ‰, average value –28.7 ‰. In the CS liquid pyrolysate of the sample D16 the $\delta^{13}C$values of individual C_{15}-C_{31} *n*-alkanes range from –27.8 to –31.1 ‰, average value –29.6 ‰. The average $\delta^{13}C$ values of *n*-alkanes in liquid pyrolysates from the CS show an increase of ~ 3 ‰ in comparison to initial bitumen in the sample D13, and ~ 1 ‰ in the sample D16. In relation to liquid pyrolysates from the OS, liquid pyrolysates from the CS has significant enrichment in heavier isotope ^{13}C, ~ 5 ‰ in the sample D13 and ~ 3 ‰ in the D16. Clearly, more intense thermal stress in the CS leads to the increase cleavage of carbon bonds containing ^{13}C, resulting in higher $\delta^{13}C$ values of *n*-alkanes. Therefore, $\delta^{13}C$ data of samples of different maturity and particularly, of liquid products obtained by different system pyrolysis should be used with caution.

Comparing carbon isotope curves of individual *n*-alkanes in initial bitumen and liquid pyrolysates from the open and closed systems of both samples (Fig. 7) it is noticeable that they are not similar but they have the same trend (OS < bitumen < CS). Pyrolytic experiments show that the isotopic ratio of *n*-alkanes obtained by the OS becomes isotopically lighter in comparison to bitumen, while in liquid products from the CS they become heavier. In the CS, thermal processes are more intense and cause decomposition of resistant aliphatic biopolymers derived from algae, which are enriched in ^{13}C isotope (Collister et al., 1994; Love et al., 1998). The enrichment of *n*-alkanes in ^{13}C is more pronounced in CS liquid pyrolysate of the sample D13 than D16 (Fig. 7), and can be explained by kerogen type, i.e. higher contribution of algal

OM in D13 (Sections 2.1 and 3.1; Gajica et al., 2017a). In liquid products from the OS and initial bitumen mentioned isotopic signature is missing due to the insufficient thermal stress for substantial algaenan degradation during diagenesis (Collister et al., 1994; Love et al., 1998).

4. Conclusions

The comparative study of the molecular composition of aliphatic hydrocarbons, ketones and fatty acid methyl esters of initial extracted bitumen and liquid pyrolysates obtained by the open and closed pyrolysis systems of the immature oil shale samples from the Aleksinac deposit (Serbia) was done and the applicability of pyrolysis type, biomarker classes and $\delta^{13}C$ of *n*-alkanes in liquid pyrolysates was determined.

During the pyrolysis in the OS, weakly kerogen bounded biomarkers are released in form in which they were incorporated into macromolecular structure. Due to the quick removal from the reaction medium, there is no possibility for their further degradation and rearrangement into other compounds, thus enables well preservation of biomarkers' stereochemistry. Generally, liquid pyrolysates from the OS show similar distribution of biomarkers as initial bitumen of raw samples, independently on kerogen type. The biomarker data of liquid pyrolysates from the OS confirmed predominantly algal origin of OM deposited in lacustrine environment, even more evident than molecular signatures of initial bitumen. This indicates applicability of OS pyrolyisis for determination of the source and depositional environment of OM.

On the other hand, during pyrolysis in the CS cracking of kerogen occurs. The released molecules are retained in reaction medium, resulting in their further transformation and/or degradation via secondary processes. Therefore, certain biomarkers are transformed into their thermodynamically more stable counterparts or even other compounds, and consequently the source fingerprints sometimes completely disappear.

The sterane and hopane maturity parameters in liquid pyrolysates from the open system reflect the low degree of maturity, similar to initial bitumen that corresponds to late diagenetic stage. Due to the fast release from the reaction medium, biomarker distributions remained mostly unaltered, although slight thermal influence on *n*-alkane parameters and the Pr/Ph ratio is observed. Composition of liquid products from the closed pyrolysis system differs, due to the prolonged exposure of OM to thermal stress, effect of pressure and native mineral catalysts. This is reflected through the values of sterane and hopane maturity ratios, distributions of *n*-alkanes,

and absence of unsaturated compounds (alkenes, hopenes), which are abundant in liquid pyrolysates from the OS. The obtained results also indicate that *n*-alkan-2-ones and fatty acids methyl esters are applicable in interpretation up to late diagenetic stage, whereas at higher maturities their distributions are very scarce and represented by several short-chain homologues, only. The composition of liquid pyrolysates from the closed system is comparable to crude oil. It is noteworthy to notice that in the CS isomerization reactions of polycyclic biomarkers follow their trends in natural conditions (e.g. faster epimerization at chiral C-atoms in side chain than isomerization in rings). The biomarker maturity ratios are slightly higher in the closed system pyrolysis products of the sample D16 (mixed type I/II kerogen) than the sample D13 (type I kerogen).

The isotopic signatures of *n*-alkanes in liquid products obtained by the OS pyrolysis are isotopically lighter than in initial bitumen (~ 2 ‰), independently on kerogen type, whereas in liquid pyrolysates from the CS they become heavier, showing more pronounced difference for type I kerogen, enriched in ^{13}C from algal biomass. The results indicate that $\delta^{13}C$ data should be used with caution in interpretation of samples having different maturity and particularly liquid products from different pyrolytic systems.

Declaration of competing interest

The authors declare no conflict of interest. The funders had no role in the design of the study; in the collection, analyses, or interpretation of data; in the writing of the manuscript, or in the decision to publish the results.

Credit author statement

Gordana Gajica: conceptualization, formal analyses, data interpretation, writing original draft, writing the submitted version; **Aleksandra Šajnović:** conceptualization, data interpretation, writing review & editing; **Ksenija Stojanović:** conceptualization, data interpretation, writing review & editing, editing the submitted version; **Jan Schwarzbauer:** formal analysis, data interpretation, writing review & editing; **Aleksandar Kostić:** collection of the samples, geological settings, writing review & editing;. **Branimir Jovančićević:** supervision, writing review & editing. All authors gave final approval of the manuscript version to be submitted.

Acknowledgments

The authors would like to thank the Ministry of Education, Science and Technological Development of Republic of Serbia (Grant No: 451-03-9/2021-14/200026 and Contract number:

451-03-9/2021-14/200168) for financial support. We are also grateful to Professor Guangli Wang and the anonymous reviewer for useful comments and suggestions, as well as to the Section Editor, Professor Hui Tian for handling of the manuscript.

References

Adam, P., Schmid, J.C., Mycke, B., Strazielle, C., Connan, J., Huc, A., Riva, A., Albrecht, P., 1993. Structural investigations of nonpolar sulfur cross-linked macromolecules in petroleum. Geochim. Cosmochim. Acta 57, 3395–3419.

Alexander, R., Kralert, P.G., Kagi, R.I., 1992. Kinetics and mechanism of the thermal decomposition of esters in sediments. Org. Geochem. 19, 133–140.

Behar, F., Kressmann, S., Rudkiewicz, J.L., Vandenbroucke, M., 1992. Experimental simulation in a confined system and kinetic modelling of kerogen and oil cracking. Org. Geochem. 19, 173–189.

Berwick, L., Greenwood, P., Kagi, R., Croué, J., 2007. Thermal release of nitrogen organics from natural organic matter using micro scale sealed vessel pyrolysis. Org. Geochem. 38, 1073–1090.

Berwick, L.J., Greenwood, P.F., Meredith, W., Snape, C.E., Talbot, H.M., 2010. Comparison of microscale sealed vessel pyrolysis (MSSVpy) and hydropyrolysis (Hypy) for the characterization of extant and sedimentary organic matter. J. Anal. Appl. Pyrolysis 87, 108–116.

Bishop, A.N., Love, G.D., McAulay, A.D., Snape, C.E., Farrimond, P. 1998. Release of kerogen-bound hopanoids by hydropyrolysis. Org. Geochem. 29, 989–1001.

Bjorøy, M., Hall, K., Gillyon, P., Jumeau, J., 1991. Carbon isotope variations in n-alkanes and isoprenoids of whole oils. Chem. Geol. 93, 13–20.

Bowden, S.A., Farrimond, P., Snape, C.E., Love, G.D. 2006. Compositional differences in biomarker constituents of the hydrocarbon, resin, asphaltene and kerogen fractions: An example from the Jet Rock (Yorkshire, UK). Org. Geochem. 37, 369–383.

Brassell, S.C., Comet, P.A., Eglinton, G., Isaacson, P.J., McEvoy, J., Maxwell, J.R., Thompson, I.D., Tibbetts, P.J.C., Volkman, J.K., 1980. The origin and fate of lipids in the Japan Trench. In: Douglas, A.G., Maxwell, J.R. (Eds.), Advances in Organic Geochemistry 1979. Pergamon Press, Oxford, pp. 375–392.

Brassell, S.C., Lewis, C.A., de Leeuw, J.W., de Lange, F., Sinninghe Damsté, J.S., 1986. Isoprenoid thiophenes: novel products of sediment diagenesis? Nature 320, 160–162.

Cheng, B., Du, J.Y., Tian, Y.K., Liu, H., Liao, Z.W., 2016. Thermal evolution of adsorbed/occluded hydrocarbons inside kerogens and its significance as exemplified by one low-matured kerogen from Santanghu Basin, Northwest China. Energy Fuels 30, 4529–4536.

Collister, J.W., Lichtfouse, È., Hieshlma, G., Hayes, J.M., 1994. Partial resolution of sources of n-alkanes in the saline portion of the Parachute Creek Member, Green River Formation (Piceance Creek Basin, Colorado). Org. Geochem. 21, 645–659.

Comet, P.A., McEvoy, J., Giger, W., Douglas, A.G., 1986. Hydrous and anhydrous pyrolysis of DSDP Leg 75 kerogens – a comparative study using a biological marker approach. Org. Geochem. 9, 171–182.

Connan, J., 1974. Diagenese naturelle et diageneses artificielle de la matiere organique a element vegetaux predominant. In: Tissot, B.P., Bienner, F. (Eds.), Advances in Organic Geochemistry 1973. Éditions Technip, Paris, pp. 73–95.

Cranwell, P.A., 1984. Lipid geochemistry of sediments from Upton Broad, a small productive lake. Org. Geochem. 7, 25–37.

Cranwell, P.A., Eglinton, G., Robinson, N., 1987. Lipids of aquatic organisms as potential contributors to lacustrine sediments-II. Org. Geochem. 6, 513–527.

de Leeuw, J.W., Cox, H.C., van Graas, G., van de Meer, F.W., Peakman, T.M., Baas, J.M.A., van de Graaf, B., 1989. Limited double bond isomerization and selective hydrogenation of sterenes during early diagenesis. Geochim. Cosmochim. Acta 53, 903–909.

De Rosa, M., Gambacorta, A., Minale, L., Bullock, J.D., 1971. Bacterial triterpenes. J. Chem. Soc. D: Chem. Comm. 12, 619–620.

Derenne, S., Largeau, C., Behar, F., 1994. Low polarity pyrolysis products of Permian to Recent Botryococcus-rich sediments: first evidence for the contribution of an isoprenoid algaenan to kerogen formation. Geochim. Cosmochim. Acta 58, 3703–3711.

Douglas, A.G., Sinninghe Damastè, J.S., Fowler, M.G., Eglinton, T.I., de Leeuw, J.W., 1990. Unique distributions of hydrocarbons and sulphur compounds released by flash pyrolysis from the fossilised alga Gloeocapsomorpha prisca, a major constituent in one of four Ordovician kerogens. Geochim. Cosmochim. Acta 55, 275–291.

Dubreuil, C., Derenne, S., Largeau, C., Berkaloff, C., Rousseau, B., 1989. Mechanism of formation and chemical structure of coorongite–I. Role of the resistant biopolymer and of the hydrocarbons of Botryococcus braunii. Ultrastructure of Coorongite and its relationship with Torbanite. Org. Geochem. 14, 543–553.

El Harfi, K., Mokhlisse, A., Chana, M.B., Outzourhit, A., 2000. Pyrolysis of the Moroccan (Tarfaya) oil shales under microwave irradiation. Fuel 79, 733742.

Ercegovac, M., Grgurović, D., Bajc, S., Vitorović, D., 2003. Oil shale in Serbia: geological and chemical-technological investigations, actual problems of exploration and feasibility studies. In: Vujić, S. (Ed.), Mineral material complex of Serbia and Montenegro at the crossings of two millenniums. Margo-Art, Belgrade, pp. 368–378.

Farrimond, P., Love, G.D., Bishop, A.N., Innes, H.E., Watson, D.F., Snape, C.E. 2003. Evidence for the rapid incorporation of hopanoids into kerogen. Geochim. Cosmochim. Acta 67, 1383–1394.

Farrimond, P., Taylor, A., Telnæs, N., 1998. Biomarker maturity parameters: the role of generation and thermal degradation. Org. Geochem. 29, 1181–1197.

Ficken, K.J., Li, B., Swain, D.L., Eglinton, G., 2000. An n-alkane proxy for the sedimentary input of submerged/floating freshwater aquatic macrophytes. Org. Geochem. 31, 745–749.

Franco, N., Kalkreuth, W., Peralba, M.C.R.P., 2010. Geochemical characterization of solid residues, bitumen and expelled oil based on steam pyrolysis experiments from Irati oil shale, Brazil: A preliminary study. Fuel 89, 1863–1871.

Freeman, K.H., Hayes, J.M., Trendel, J.M., Albrecht, P., 1990. Evidence from carbon isotope measurement for diverse origins of sedimentary hydrocarbons. Nature 343, 254–256.

Gajica, G., Šajnović, A., Stojanović, K., Antonijević, M., Aleksić, N., Jovančićević, B., 2017b. The influence of pyrolysis type on shale oil generation and its composition (Upper layer of Aleksinac oil shale, Serbia). J. Serb. Chem. Soc. 82, 1461–1477.

Gajica, G., Šajnović, A., Stojanović, K., Kostić, A., Slipper, I., Antonijević, M., Nytoft, H.P., Jovančićević, B., 2017a. Organic geochemical study of the upper layer of Aleksinac oil shale in the Dubrava block, Serbia. Oil Shale 34, 197–218.

Gelin, F., Boogers, I., Noordeloos, A.A.M., Sinninghe Damsté, J.S., Riegman, R., de Leeuw, J.W., 1997. Resistant biomacromolecules in marine microalgae of the classes Eustigmatophyceae and Chlorophyceae: geochemical implications. Org. Geochem. 26, 659–675.

Gelin, F., Gatellier, J.-P.L.A., Sinninghe Damsté, J.S., Metzger, P., Derenne, S., Largeau, C., de Leeuw, J.W., 1993. Mechanisms of flash pyrolysis of ether lipids isolated from the green microalga Botryococcus braunii race A. J. Anal. Appl. Pyrol. 27, 155–168.

Gelpi, E., Oró, J., Schneider, H.J., Bennett, E.O., 1968. Olefins of high molecular weight in two microscopic algae. Science 161, 700–702.

González-Vila, F.J., Polvillo, O., Boski, T., Moura, D., de Andreés, J.R., 2003. Biomarker patterns in a time-resolved Holocene/terminal Pleistocene sedimentary sequence from the Guadiana river estuarine area (SW Portugal/Spain border). Org. Geochem. 34, 1601–1613.

Goossens, H., de Leeuw, J.W., Schenck, P.A., Brassell, S.C., 1984. Tocopherols as likely precursors of pristane in ancient sediments and crude oils. Nature 312, 440–442.

Grice, K., Schouten, S., Blokker, P., Derenne, S., Largeau, C., Nissenbaum, A., Sinninghe Damsté, J.S., 2003. Structural and isotopic analysis of kerogens in sediments rich in free sulfurised Botryococcus braunii biomarkers. Org. Geochem. 34, 471–482.

Hakimi, M.H., Abdullah, W.H., Alqudah, M., Makeen, Y.M., Mustapha, K.A., Hatem B.A., 2018. Pyrolysis analyses and bulk kinetic models of the Late Cretaceous oil shales in Jordan and their implications for early mature sulphur-rich oil generation potential. Mar. Pet. Geol. 91, 764–775.

Hatem, B.A., Abdullah, W.H., Hakimi, M.H., Mustapha, K.A., 2016. Origin of organic matter and paleoenvironment conditions of the Late Jurassic organic-rich shales from shabwah sub-basin (western Yemen): Constraints from petrology and biological markers. Mar. Pet. Geol. 72, 83–97.

Hofmann, I.C., Hutchinson, J., Robson, J.N., Chicarelli, M.I., Maxwell, J.R., 1992. Evidence for sulphide links in a crude oil asphaltene and kerogens from reductive cleavage by lithium in ethylamine. Org. Geochem. 19, 371–387.

Holba, A.G., Tegelaar, E.W., Huizinga, B.J., Moldowan, J.M., Singletary, M.S., McCaffrey, M.A., Dzou, L. I. P., 1998. 24-norcholestanes as age-sensitive molecular fossils. Geology 26, 783–786.

Höld, I.M., Schouten, S., Van der Gaast, S.J., Sinninghe Damsté, J.S., 2001. Origin of prist-1-ene and prist-2-ene in kerogen pyrolysates. Chem. Geol. 172, 201–212.

Ingram, L.L., Ellis, J., Crisp, P.T., Cook, A.C., 1983. Comparative study of oil shales and shale oils from the mahogany zone, Green River Formation (U.S.A.) and Kerosene Creek seam, Rundle Formation (Australia). Chem. Geol. 38, 185–212.

Ishiwatari, R., Ishiwatari, M., 2004. Insights on the origin of pristane and phytane in sediments and oils from laboratory heating experiments. Geochem. Soc. Spec. Publ. 9, 85–96.

Jelenković, R., Kostić, A., Životić, D., Ercegovac, M., 2008. Mineral resources of Serbia. Geol. Carpath. 59, 345–361.

Kissin, Y.V., 1993. Catagenesis of light acyclic isoprenoids in petroleum. Org. Geochem. 20, 1077–1090.

Klink, G., Dreier, F., Buchs, A., Giilaqar, F.O., 1992. A new source for 4-methyl sterols in freshwater sediments: Utricularia neglecta L. (Lentibulariaceae). Org. Geochem. 18, 757–763.

Larter, S.R., Solli, H., Douglas, A.G., de Lange, F., de Leeuw, J.W., 1979. Occurrence and significance of prist-1-ene in kerogen pyrolysates. Nature 279, 405–408.

Leif, N.R., Simoneit, B.R.T., 2000. The role of alkenes produced during hydrous pyrolysis of a shale. Org. Geochem. 31, 1189–1208.

Lewan, M. D., 1983. Effects of thermal maturation on stable organic carbon isotopes as determined by hydrous pyrolysis of Woodford Shale. Geochim. Cosmochim. Acta 47, 1471–1479.

Lewan, M.D., 1998. Sulphur-radical control on petroleum formation rates. Nature 391, 164–166.

Lewan, M.D., Bjorøy, M., Dolcater, D.L., 1986. Effects of thermal maturation on steroid hydrocarbons as determined by hydrous pyrolysis of Phosphoria Retort Shale. Geochim. Cosmochim. Acta 50, 1977–1987.

Li, M., Jiang, C., 2001. Bakken/Madison petroleum systems in the Canadian Williston Basin. Part 1: C21–C26 20-n-alkylpregnanes and their triaromatic analogs as indicators for Upper Devonian–Mississippian epicontinental black shale derived oils? Org. Geochem. 32, 667–675.

Lichtfouse, È., Derenne, S., Mariotti, A., Largeau, C., 1994. Possible algal origin of long chain odd n-alkanes in immature sediments as revealed by distributions and carbon isotope ratios. Org. Geochem. 22, 1023–1027.

Liu, W., Yang, H., Wang, H., An, Z., Wang, Z., Leng, Q., 2015. Carbon isotope composition of long chain leaf wax n-alkanes in lake sediments: A dual indicator of paleoenvironment in the Qinghai-Tibet Plateau. Org. Geochem. 83-84, 190–201.

Lockhart, R.S., Meredith, W., Love, G.D., Snape, C.E., 2008. Release of bound aliphatic biomarker via hydropyrolysis from Type II kerogen at high maturity. Org. Geochem. 39, 1119–1124.

Love, G.D., Bowden, S.A., Jahnke, L.L., Snape, C.E., Campbell, J.G., Day, J.G., Summons, R.E., 2005. A catalytic hydropyrolysis method for the rapid screening of microbial cultures for lipid biomarkers. Org. Geochem. 36, 63–82.

Love, G.D., Colin, E.S, Fallick, A.E., 1998. Differences in the mode of incorporation and biogenicity of the principal aliphatic constituents of a Type I oil shale. Org. Geochem. 28, 797–811.

Love, G.D., McAulay, A., Snape, C.E., Bishop, A.N., 1997. Effect of process variable in catalytic hydropyrolysis on the release of bound aliphatic hydrocarbons from sedimentary organic matter. Energy Fuels 11, 522–531.

Love, G.D., Snape, C.E., Carr, A.D., Houghton, R., 1995. Release of bound alkane biomarkers in high yields from kerogen via catalytic hydropyrolysis. Org. Geochem. 23, 981–986.

Lu, H., Chen, T., Grice, K., Greenwood, P., Peng, P., Sheng, G., 2009. Distribution and significance of novel low molecular weight sterenes in an immature evaporitic sediment from the Jinxian Sag, North China. Org. Geochem. 40, 902–911.

Lu, S.-T., Kaplan, I.R., 1992. Diterpanes, triterpanes, steranes, and aromatic hydrocarbons in natural bitumens and pyrolysates from different humic coals. Geochim. Cosmochim. Acta 56, 2761–2788.

Meredith, W., Snape, C.E., Carr, A.D., Nytoft, H.P., Love, G.D., 2008. The occurrence of unusual hopanes in hydropyrolysates generated from severely biodegraded oil seep asphaltenes. Org. Geochem. 39, 1243–1248.

Merritt, M.V., Rosenstein, S.P., Loh, C., 1991. A comparison of the major lipid classes and fatty acids composition of marine unicellular cyanobacteria with freshwater species. Arch. Microbiol. 155, 107–113.

Monthioux, M., Landais, P., Monin, J.-C., 1985. Comparison between natural and artificial maturation series of humic coals from the Mahakam delta. Org. Geochem. 8, 275–292.

Murray, I.P., Love, G.D., Snape, C.E., Bailey, N.J.L., 1998. Comparison of covalently-bound aliphatic biomarkers released via hydropyrolysis with their solvent-extractable counterparts for a suite of Kimmeridge clays. Org. Geochem. 29, 1487–1505.

Neto, E.V., Hayes, J.M., Takaki, T., 1998. Isotopic biogeochemistry of the Neocomian lacustrine and Upper Aptian marine-evaporitic sediments of the Potiguar Basin, Northeastern Brazil. Org. Geochem. 28, 361–381.

Ourisson, G., Albrecht, P., Rohmer, M., 1979. The hopanoids: palaeo-chemistry and biochemistry of a group of natural products. Pure Appl. Chem. 51, 709–729.

Pakdel, H., Roy, C., Kalkreuth, W., 1999. Oil production by vacuum pyrolysis of Canadian oil shales and fate of the biological markers. Fuel 78, 365–375.

Pan, C., Zhang, M., Peng, D., Yu, L., Liu, J., Sheng, G., Fu, J., 2010. Confined pyrolysis of Tertiary lacustrine source rocks in the Western Qaidam Basin, Northwest China: Implications for generative potential and oil maturity evaluation. Appl. Geochem. 25, 276–287.

Perunović, T., Stojanović, K., Simić, V., Kašanin-Grubin, M., Šajnović, A., Erić, V., Schwarzbauer, J., Vasić, N., Jovančićević, B., Brčeski, I., 2014. Organic geochemical study of the lower Miocene Kremna basin, Serbia. Ann. Soc. Geol. Pol. 84, 185–212.

Peters, K.E., Moldowan, J.M., Sundararaman, P., 1990. Effects of hydrous pyrolysis on biomarker thermal maturity parameters: monterey phosphatic and siliceous members. Org. Geochem. 15, 249–265.

Peters, K.E., Walters, C.C., Moldowan, J.M., 2005. The Biomarker Guide, Vol. 2: Biomarkers and Isotopes in Petroleum Exploration and Earth History, Second edition. Cambridge University Press, Cambridge.

Philp, R.P., 1987. A review of biomarkers in kerogens as determined by pyrolysis-gas chromatography and pyrolysis-gas chromatography-mass spectrometry. J. Anal. Appl. Pyrol. 11, 93–108.

Rampen, S.W., Schouten, S., Panoto, F.E., Muyzer, G., Campbell, C.N., Fehling, J., Sinninghe Damsté, J.S., 2007. On the origin of 24-norcholesanes and their use as age-diagnostic biomarkers. Geology 35, 419–422.

Reynolds, J. G., Burnham, A. K., Mitchell, T.O. 1995. Kinetic analysis of California petroleum source rocks by programmed temperature micropyrolysis. Org. Geochem. 23, 109–120.

Rohmer, M., Bouvier-Nave, P., Ourisson, G., 1984. Distribution of hopanoid triterpenes in prokaryotes. J. Gen. Microbiol. 130, 1137–1150.

Rontani, J.-F., Baillet, G., Aubert, C., 1991. Production of cyclic isoprenoid compounds during the photodegradation of chlorophyll-α in seawater. J. Photochem. Photobiol. A: Chem. 59, 369–377.

Rontani, J.-F., Giral, P.J.-P., 1990. Significance of photosensitized oxidation of alkanes during the photochemical degradation of petroleum hydrocarbon fractions in seawater. Internat. J. Environ. Anal. Chem. 42, 61–68.

Rontani, J.-F., Volkman, J.K., 2003. Phytol degradation products as biogeochemical tracers in aquatic environments. Org. Geochem. 34, 1–35.

Rovere, C.E., Crisp, P.T., Ellis, J., Bolton, P.D., 1983. Chemical characterization of shale oil from Condor, Australia. Fuel 62, 1274–1282.

Rubinstein, I., Spyckerelle, C., Strausz, O.P., 1979. Pyrolysis of asphaltenes: a source of geochemical information. Geochim. Cosmochim Acta 43, 1–6.

Rullkötter, J., Marzi, R., 1988. Natural and artificial maturation of biological markers in a Toarcian shale from northern Germany. Org. Geochem. 13, 639–645.

Russell, R.A., Snape, C.E., Meredith, W., Love, G.D., Clarke, E., Moffatt, B., 2004. The potential of bound biomarker profiles released via catalytic hydropyrolysis to reconstruct basin charging history for oils. Org. Geochem. 35, 1441–1459.

Schidlowski, M., 1986. 13C/12C ratios as indicators of biogenicity. In: Johns, R.B. (Ed.), Biological Markers in the Sedimentary Record. Elsevier, Amsterdam, pp. 347-361.

Schwarzbauer, J., Littke, R., Meier, R., Strauss, H., 2013. Stable carbon isotope ratios of aliphatic biomarkers in Late Palaeozoic coals. Int. J. Coal Geol. 107, 127–140.

Seifert, W. K., Moldowan, J. M., 1980. The effect of thermal stress on source-rock quality as measured by hopane stereochemistry. Phys. Chem. Earth, 12, 229–237.

Sert, M., Ballice, L., Yüksel, M., Sağlam, M., 2009. Effect of mineral matter on product yield and composition at isothermal pyrolysis of Turkish oil shales. Oil Shale 26, 463–474.

Sinninghe Damsté, J.S., de las Heras, F.X.C., van Bergen, P.F., de Leeuw, J.W., 1993. Characterization of Tertiary Catalan lacustrine oil shales: discovery of extremely organic sulphur-rich Type I kerogens. Geochim. Cosmochim. Acta 57, 389–415.

Snowdon, L.R., Volkman, J.K., Zhang, Z.R., Tao, G.L., Liu, P., 2016. The organic geochemistry of asphaltenes and occluded biomarkers. Org. Geochem. 91, 3–15.

Stasiuk, L.D, 1993. Oil-prone alginite macerals from organic-rich Mesozoic and Palaeozoic strata, Saskatchewan, Canada. Mar. Pet. Geol. 11, 208–217.

Stojanović, K., Šajnović, A., Sabo, T.J., Golovko, A., Jovančićević, B., 2010. Pyrolysis and catalyzed pyrolysis in the investigation of a Neogene shale potential from Valjevo-Mionica basin, Serbia. Energy Fuel 24, 4357–4368.

Stojanović, K., Životić, D., 2013. Comparative study of Serbian Miocene coals – insights from biomarker composition. Int. J. Coal Geol. 107, 3–23.

Stojanović, K., Životić, D., Šajnović, A., Cvetković, O., Nytoft, H.P., Scheeder, G., 2012. Drmno lignite field (Kostolac Basin, Serbia): origin and palaeoenvironmental implications from petrological and organic geochemical studies. J. Serb. Chem. Soc. 77, 1109–1127.

Strizhakova, Y.A., Usova, T.V., 2008. Current Trends in the Pyrolysis of Oil Shale, Review. Solid Fuel Chem. 42, 197–201.

Strobl, S.A.I, Sachsenhofer R. F., Bechtel A., Gratzer R., Gross D., Bokhari S. N.H., Liu R., Liu Z., Meng Q., Sun P., 2014. Depositional environment of oil shale within the Eocene Jijuntun Formation in the Fushun Basin (NE China). Mar. Pet. Geol. 56, 166–183.

Sugden, M.A., Tabolt, H.M. Farrimond, P., 2005. Flash pyrolysis – a rapid method for screening bacterial species for the presence of bacteriohopanepolyols. Org. Geochem. 36, 975–979.

Šaban, M., Porter, S., Costello, C., Djuričić, M., Vitorović, D., 1980. Polar constituents isolated from the Aleksinac oil shale. In: Douglas, A.G., Maxwell, J.R. (Eds.), Advances in Organic Geochemistry 1979. Pergamon Press, Oxford, pp. 559–566.

ten Haven, H.L., de Leeuw, J.W., Peakman, T.M., Maxwell, J.R., 1986. Anomalies in steroid and hopanoid maturity indices. Geochim. Cosmochim. Acta 50, 853–855.

Tian, C., Xia, Y., Song, C., Ma, S., Gao, W., Xing, L., 2017. Changes in the carbon isotope composition of pristane and phytane with increasing maturity. Pet. Sci. Technol. 35, 1270–1276.

Tissot, B.P., Welte, D.H., 1984. Petroleum Formation and Occurrence, 2nd Ed. Springer-Verlag, Berlin.

Tuo, J., Li Q., 2005. Occurrence and distribution of long-chain acyclic ketones in immature coals. Appl. Geochem. 20, 553–568.

van de Meent, D., de Leeuw, J.W., Schenck, P.A., 1980. Origin of unsaturated isoprenoid hydrocarbons in pyrolysates of suspended matter and surface sediments. In: Douglas, A.G., Maxwell, J.R. (Eds.), Advances in Organic Geochemistry. Pergamon Press, Oxford, pp. 469–474.

Volkman, J K., 1986. A review of sterol markers for marine and terrigenous organic matter. Org. Geochem. 9, 83–99.

Volkman, J.K., 2014. Acyclic isoprenoid biomarkers and evolution of biosynthetic pathways in green algae of the genus Botryococcus. Org. Geochem. 75, 36–47.

Volkman, J.K., Farrington, J.W., Gagosian, R.B., Wakeham, S.G., 1983. Lipid composition of coastal marine sediments from the Peru upwelling region. In: Bjoroy, M., Albrecht, P., Cornford, C. (Eds.), Advances in Organic Geochemistry 1981. John Wiley and Sons, New York, pp. 228–240.

Volkman, J.K., Zhang, Z., Xie, X., Qin, J., Borjigin, T., 2015. Biomarker evidence for Botryococcus and a methane cycle in the Eocene Huadian oil shale, NE China. Org. Geochem. 78, 121–134.

Vu, T.A.T., Horsfield, B., Sykes, R., 2008. Influence of in-situ bitumen on the generation of gas and oil in New Zealand coals. Org. Geochem. 39, 1606–1619.

Vuković, N., Životić, D., Mendonça Filho, J.G., Kravić-Stevović, T., Hámor-Vidó, M., de Oliveira Mendonça, J., Stojanović, K., 2016. The assessment of maturation changes of humic coal organic matter - Insights from closed-system pyrolysis experiments. Int. J. Coal Geol. 154–155, 213–239.

Wang, X.Z., Song, Y.T., Wang, X.J., 1996. Petroleum Formation and Expulsion by Simulation. Petroleum University Press, Dongying. (in Chinese).

Wang, G., Wang, T.-G., Simoneit, B.R.T., Chen, Z., Zhang, L., Xu, J., 2008. The distribution of molecular fossils derived from dinoflagellates in Paleogene lacustrine sediments (Bohai Bay Basin, China). Org. Geochem. 39, 1512–1521.

Wang, G., Wang, T.-G., Simoneit, B.R.T., Zhang, L., Zhang, X., 2010. Sulfur rich petroleum derived from lacustrine carbonate source rocks in Bohai Bay Basin, East China. Org. Geochem. 41, 340–354.

Wingert, W.S., Pomerantz, M., 1986. Structure and significance of some twenty-one and twenty-two carbon petroleum steranes. Geochim. Cosmochim. Acta 50, 2763–2769.

Wolff, G.A., Lamb, N.A., Maxwell, J.R., 1986. The origin and fate of 4-methyl steroid hydrocarbons. I. Diagenesis of 4-methyl sterenes. Geochim. Cosmochim. Acta 50, 335–342.

Wu, L., Geng, A., 2016. Differences in the thermal evolution of hopanes and steranes in free and bound fractions. Org. Geochem. 101, 38–48.

Wu, L., Horsfield, B., 2019. Initial insights into releasing bound biomarkers from kerogen matrices using microscale sealed vessel catalytic hydrogenation (MSSV-HY). Org. Geochem. 130, 22–32.

Wu, L.L., Liao, Y.H., Fang, Y.X., Geng, A.S., 2013. The comparison of biomarkers released by hydropyrolysis and Soxhlet extraction from source rocks of different maturities. Chin. Sci.Bull. 58, 373–383.

Ying, G.G., Fan, P., 1993. Origin of ketones in sediments of Qinghai Lake. Sci. China. Ser. B: Chem. 36, 237–241.

Yoshioka, H., Ishiwatari, R., 2002. Characterization of organic matter generated from Green River shale by infrared laser pyrolysis. Geochem. J. 36, 73–82.

Zhang, T., Wang, Z., Wang, X., Peng, Liu P., Wang, Y., Wu, Y., 2021. Characterization of oxygen-bearing geolipids in the Upper Permian Lucaogou shale, Santanghu Basin, NE China, using stepwise pyrolysis and hydrous pyrolysis. Mar. Pet. Geol. 126, 104926.

Zhang, Z., Volkman, J.K., 2017. Algaenan structure in the microalga Nannochloropsis oculata characterized from stepwise pyrolysis. Org. Geochem. 104, 1–7.

Zhang, Z., Volkman, J.K., Xie, X, Snowdon, L.R., 2016. Stepwise pyrolysis of the kerogen from the Huadian oil shale, NE China: Algaenan-derived hydrocarbons and mid-chain ketones. Org. Geochem. 91, 89–99.

Highlights

- Open system pyrolysis is useful for determination of organic matter sources, independently on kerogen type.
- Pyrolysis of oil shale in closed system generates liquid product comparable to crude oil.
- Mixed type I/II kerogen attained slightly higher maturity than type I kerogen by closed system pyrolysis.
- $\delta^{13}C$ of individual *n*-alkanes displayed notable variations depending on pyrolysis type.